

Operator Growth in Disordered Spin Chains: Indications for the Absence of Many-Body Localization

A. Weisse

Max-Planck-Institut für Mathematik, Vivatsgasse 7, 53111 Bonn, Germany

R. Gerstner and J. Sirker

Department of Physics and Astronomy and Manitoba Quantum Institute,

University of Manitoba, Winnipeg, Canada R3T 2N2

(Dated: July 16, 2024)

We consider the growth of a local operator A in one-dimensional many-body systems with Hamiltonian H by calculating the k -fold commutator $[H, [H, [\dots, [H, A]]]]$. We derive general bounds for the operator norm of this commutator in free and interacting fermionic systems with and without disorder thus directly connecting the *operator growth hypothesis* with questions of localization. We show, in particular, that in a localized system the norm does grow at most exponentially and that the contributions of operators to the total norm are exponentially suppressed with their length. We support our general results by considering one specific example, the XXZ chain with random magnetic fields. We solve the operator spreading in the XX case without disorder exactly. For the Anderson and Aubry-André models we provide strict upper bounds. We support our results by symbolic calculations of the commutator up to high orders. For the XXX case with random magnetic fields, these symbolic calculations show a growth of the operator norm faster than exponential and consistent with the general bound for an ergodic system. Also, there is no exponential decay of the contribution of operators as function of their length. We conclude that there is no indication for a many-body localization transition. Finally, we also discuss the differences between the interacting and non-interacting cases when trying to perturbatively transform the microscopic to an effective Hamiltonian of local conserved charges by consecutive Schrieffer-Wolff transformations. We find that such an approach is not well-defined in the interacting case because the transformation generates $\sim 4^\ell$ terms connecting sites a distance ℓ apart which can overwhelm the exponential decay with ℓ of the amplitude of each individual term.

I. INTRODUCTION

In a one-dimensional fermionic lattice model with short-range hoppings and without interactions, any amount of disorder leads to a localization of the eigenfunctions. This is known as Anderson localization [1–4]. An open question for the last 65 years has been what happens if interactions are included. One of the difficulties in investigating this question is that localization can no longer be defined in terms of single-particle eigenfunctions; new indicators of localization are needed.

Studying the possibility of localization in the many-body case has gained renewed interest in the last 17 years starting with the work by Basko, Aleiner, and Altshuler [5]. This was followed by a large number of numerical studies concentrating, in particular, on the Heisenberg (XXX) chain with random magnetic fields [6–19]. By a Jordan-Wigner transform, this model is equivalent to a fermionic chain with nearest-neighbor hoppings, density-density interactions, and random on-site potentials. Based on an analysis of spectral properties such as the level spacing as well as of dynamical properties such as the growth of the entanglement entropy after a quantum quench from an unentangled initial state, an apparent consensus was reached that this model shows a phase transition in all eigenstates at a finite disorder strength, separating an ergodic from a many-body localized phase. This consensus was first called into question

by studies showing that the transition point, defined for a finite system of size L , appears to slowly shift to infinite disorder strength for $L \rightarrow \infty$ [20, 21]. These arguments were supported by studies of the number entropy after a quantum quench [22–27] and of the fidelity susceptibility [28, 29].

Here we want to propose and follow a new avenue by studying the properties of operators instead of wave functions. Our motivation is the following observation: In an Anderson localized model, the projectors onto the eigenstates $P_n = |E_n\rangle\langle E_n|$ are conserved *quasi-local operators*, i.e., they are centered at a site in the lattice and decay exponentially away from this site. These operators are also often called local integrals of motion (LI-OMs). Without loss of generality, we can order the operators such that P_n is an operator localized around lattice site n . To be more precise, we can use the fermionic language in which the Anderson Hamiltonian and any unitary transformation of this Hamiltonian are bilinear. We can then write $P_n = \sum_{ij} a_{ij}^n c_i^\dagger c_j$ where $c_i^{(\dagger)}$ is a fermionic annihilation (creation) operator at site i and $|a_{ij}^n| \sim \exp(|i - n|) \exp(|j - n|)$ are amplitudes. In particular, the contribution of bilinear operators to P_n is exponentially suppressed with the distance they cover.

There is a unitary transformation U which diagonalizes the microscopic, non-interacting Anderson Hamiltonian H , bringing it into the form $\tilde{H} = U H U^{-1} = \sum_n E_n P_n$ where P_n is quasi-local and conserved, $[H, P_n] = 0$. Im-

portantly, this unitary transformation itself is quasi-local and will always map local microscopic operators A_i onto quasi-local operators, $\tilde{A}_i = UA_iU^{-1}$. As we will show, this has important implications for the spreading of a local operator in Euclidean time. We can write

$$\begin{aligned} A_i(\tau) &= e^{\tau H} A_i e^{-\tau H} \\ &= \sum_{k=0}^{\infty} \underbrace{[H, [H, [\dots, [H, A_i]]]]}_{k\text{-times}} \frac{\tau^k}{k!}. \end{aligned} \quad (\text{I.1})$$

I.e., the spreading of the operator is encoded in the k -fold commutator $[H, A_i]^{(k)}$ with the Hamiltonian. It is important to note that the Frobenius norm of this commutator is not affected by the unitary transformation $\| [H, A_i]^{(k)} \|_2 = \| [\tilde{H}, \tilde{A}_i]^{(k)} \|_2$. For the latter we expect that the norm of operators in the commutator which cover a distance of l sites is exponentially suppressed with l at fixed order k . As we will show, this implies that the total norm of all terms in the commutator can only grow exponentially with k .

In a many-body localized phase, it has been argued that—similar to the Anderson case—a unitary transformation of the microscopic Hamiltonian H to a Hamiltonian \tilde{H} of conserved quasi-local charges exists. The main difference is assumed to be that these quasi-local charges τ_n^z are interacting with each other [17, 19]

$$\tilde{H} = \sum_n E_n \tau_n^z + \sum_{i,j} J_{ij} \tau_i^z \tau_j^z + \dots \quad (\text{I.2})$$

Here, J_{ij} are exponentially decaying coupling constants which describe a slow dephasing between the conserved charges. For the Anderson case, $J_{ij} = 0$ and the τ_n^z can be chosen to be the projection operators P_n . We note that the choice of the quasi-local conserved operators τ_n^z is not unique. We will argue in the following that in the interacting case a local operator in the microscopic model should also remain local, up to exponential tails, under Euclidean time evolution as in the non-interacting case. This implies, in particular, that the total norm *in both cases* should at most grow exponentially with k .

This has to be contrasted with the general, ergodic case. In one dimension, there is no phase transition in a clean system at finite temperatures. Thus, the time evolution is always analytic and Eq. (I.1) implies that the norm of the k -fold commutator $[H, A_i]^{(k)}$ has to grow slower than factorially. In Ref. [30], it has been shown that this is indeed the case, however, the derived bound for the total norm grows much faster than exponential and almost factorially, $\| [H, A_i]^{(k)} \|_2 \sim (k/\ln k)^k$. The *operator growth hypothesis* states that any generic quantum chaotic system will asymptotically saturate this bound [30, 31]. Thus, we have a sharp contrast between the growth of the operator norm of the k -fold commutator of a local operator with the Hamiltonian between a localized, non-ergodic system, where it can grow at most exponentially, and a non-localized system, where an almost factorial growth is expected in general. This qualitative difference in the operator norm growth is what

we will investigate here. To avoid misunderstandings, we want to stress already here that what we mean by a local operator and what we will investigate in the following is an operator A_i which resides on lattice site i in the microscopic model. In contrast, operators of the form $A = \sum_i A_i$ are also often called local conserved charges if $[H, A] = 0$ and are of particular importance in integrable models. Operators of the type A , which are sums of local densities but which extend over the entire lattice, are also the type of operators whose growth has been investigated in Refs. [31, 32]. The latter type of operators are not of interest for a study of localization and we will not consider them here.

We note that in contrast to real-time evolution, the Euclidean time evolution of operators can be directly connected to questions of quantum chaos and the eigenstate thermalization hypothesis (ETH) [30, 31]. First, the Frobenius norm of a local operator A under Euclidean time evolution in the energy eigenbasis for a finite system of size L is given by

$$\| A(\tau) \|_2^2 = \frac{\text{tr}(A^\dagger(\tau) A(\tau))}{\text{tr} \mathbb{1}} = \sum_{ij} e^{\tau(E_i - E_j)} \frac{|A_{ij}|^2}{\text{tr} \mathbb{1}}. \quad (\text{I.3})$$

For a system satisfying ETH, most matrix elements A_{ij} are expected to be non-zero even for extensive energy differences $|E_i - E_j|$. This implies that $\| A(\tau) \|_2^2 \sim \exp(J\tau L)$ where J is the local energy scale. If a system is non-interacting or has local conservation laws on the other hand, and thus does not satisfy ETH, matrix elements will be zero for extensive energy differences and we thus expect $\| A(\tau) \|_2^2 \sim \exp(J\tau)$. By deriving strict bounds directly for the Frobenius norm $\| A(\tau) \|_2$, one can use Eq. (I.3) to make precise statements about the scaling of off-diagonal matrix elements A_{ij} as a function of $|E_i - E_j|$. For the generic, chaotic case this scaling has been considered in Ref. [30] and is consistent with numerical investigations [33, 34].

Another quantity which can be obtained from considering the Euclidean time evolution of local operators are Lieb-Robinson bounds. A clean, one-dimensional system with short-range interactions shows a linear spreading of information under real-time evolution independent of whether the system is chaotic or not [35, 36]. In contrast, under Euclidean time evolution information spreads exponentially fast, $\ell \sim e^\tau$, over a distance ℓ in a 1D chaotic system [30] while it only spreads ballistically in a non-interacting system or a system with local conservation laws. It has also been speculated that the time for the spreading of information in Euclidean time in a 1D chaotic system, $\tau \sim \ln(\ell)$, is indicative of the Thouless time in a system without conservation laws (for example a Floquet system), i.e., the time after which the system can be described by a random matrix. Furthermore, it is also possible to connect the characteristic time of Euclidean operator growth with the delocalization of this operator in Krylov space [31]. Overall, there is strong evidence that in a quantum chaotic system, an operator

grows asymptotically at its maximally allowed rate and that a parametrically slower growth is related to ergodicity breaking.

Here we want to expand the study of operator growth to disordered systems. There is, in particular, a direct conflict between the operator growth hypothesis which suggests that an almost factorial growth is indicative of ergodicity and systems such as the random transverse Ising model which has been suggested to have a many-body localized phase but does always show almost factorial operator growth [37]. While we will consider Lieb-Robinson bounds and the decay of off-diagonal matrix elements in App. B and App. C, it is important to note that these quantities are obtained by taking sums over k -fold commutators $[H, A_i]^{(k)}$ and thus some of the information, in particular about the spatial support of such commutators which is relevant for the question of localization, is lost. Here we follow a novel path by directly obtaining analytical results for the asymptotic scaling of k -fold commutators resolved by the extent of their spatial support. Our results resolve the above mentioned conflict and suggest that the operator growth hypothesis is valid and that many-body systems, even for strong disorder, do not localize but rather stay ergodic.

In addition to these analytical results, we will also present exact results from symbolic calculations of commutators and norms. To be able to consider high orders k in the commutator, we have written code in Julia with Nemo [38] which is able to handle symbolic computations with up to ~ 200 million terms, limited only by the available memory. Nemo also provides arbitrary precision complex ball arithmetic which tracks error bounds rigorously. We typically use 200 or 400 digit precision for the amplitudes of the operators. While the absolute errors for large commutator orders can become large, we keep the relative errors always below 10^{-50} such that error bars are not visible in many of the plots presented in the following. We note that by using symbolic calculations we are able to consider system sizes for nearest-neighbor models which are about twice as large as the ones typically considered in exact diagonalizations.

Our paper is organized as follows: In Sec. II, we discuss general bounds for the growth of the norm $\| [H, A]^{(k)} \|$ for a local operator A and a nearest-neighbor Hamiltonian H . We review the result in the general interacting case without localization [30] before discussing the free-fermion case and the case of localization. In Sec. III, we then consider a specific model, the XXZ spin chain. We start with the free-fermion (XX) model without disorder before discussing the Anderson case of quenched disorder. We also consider the Aubry-André model which has a periodic potential incommensurate with the lattice and shows a phase transition at a finite disorder strength which, as we will demonstrate, is clearly visible in the norm growth. We then turn to the interacting Heisenberg (XXX) model and show that results obtained by symbolic computations are inconsistent with localization for all studied disorder strengths. In Sec. IV, we con-

sider Schrieffer-Wolff transformations which can be used to perturbatively transform the Hamiltonian into a basis of quasi-local conserved operators. We show that such a perturbative construction succeeds in the non-interacting case while it will typically fail once interactions are included. The final section contains a summary of our main results and a discussion of the remaining open issues.

II. BOUNDS ON OPERATOR NORM GROWTH

We want to consider how the norm of the k -th order commutator

$$[H, A]^{(k)} \equiv \underbrace{[H, [H, [\dots, [H, A]]]]}_{k\text{-times}} \quad (\text{II.1})$$

between a one-dimensional lattice Hamiltonian

$$H = \sum_I h_{I, I+1} \equiv \sum_I h_I \quad (\text{II.2})$$

which acts only locally at nearest-neighbor sites I and $I + 1$ and a one-site operator A grows with the order of the commutator k . We consider the Hamiltonian as acting on L lattice sites which therefore can be described by an $M \times M$ matrix

$$H = \sum_I \mathbb{1}_1 \otimes \dots \otimes \mathbb{1}_{I-1} \otimes h_{I, I+1} \otimes \mathbb{1}_{I+2} \otimes \dots \otimes \mathbb{1}_L \quad (\text{II.3})$$

with $M = n^L$ where n is the number of degrees of freedom per site. We place the operator A in the middle of the chain and choose chain lengths sufficiently large so that the support of $[H, A]^{(k)}$ is always less than L .

We consider two entry-wise matrix norms for a matrix A with elements A_{ij} :

$$\begin{aligned} \|A\|_1 &= \sum_{i,j} |A_{ij}| / \sqrt{\text{tr } \mathbb{1}_{M \times M}} \\ \|A\|_2 &= \sqrt{\frac{\text{tr } (A^\dagger A)}{\text{tr } \mathbb{1}_{M \times M}}} = \sqrt{\frac{\sum_{i,j} |A_{ij}|^2}{\text{tr } \mathbb{1}_{M \times M}}}. \end{aligned} \quad (\text{II.4})$$

We note that the 2-norm is also called the Frobenius norm. For finite-dimensional spaces it is also equivalent to the Hilbert-Schmidt norm which is consistent with the standard scalar product in quantum mechanics at infinite temperatures. We divide here by the constant factor $\text{tr } \mathbb{1}_{M \times M}$ such that the identity operator acting on the entire system is normalized to one. We note that the 2-norm is invariant under unitary transformations. I.e., the operator growth of a local operator A in the microscopic model with Hamiltonian H under Euclidean time evolution is exactly the same as that of the transformed operator $\tilde{A} = UAU^\dagger$ in the effective model $H_{\text{eff}} = UHU^\dagger$ if U describes a unitary transformation. The 1-norm, on the other hand, is not invariant under basis changes. Let us therefore explain how we define the matrix A corresponding to an operator. If $\{\sigma_i^\alpha\}$ is a f -dimensional local operator basis, then we can always write

$$A = \sum_{\{\alpha\}} a_{\alpha_1, \dots, \alpha_L} \sigma_1^{\alpha_1} \otimes \dots \otimes \sigma_L^{\alpha_L}. \quad (\text{II.5})$$

There are f^L many coefficients $a_{\alpha_1, \dots, \alpha_L}$, and the 2-norm is given by $\|A\|_2 = \sqrt{\sum_{\{\alpha\}} |a_{\alpha_1, \dots, \alpha_L}|^2}$. We can therefore consider as entries of our matrix A the f^L many coefficients $\sqrt{\text{tr } \mathbb{1}_{M \times M}} a_{\alpha_1, \dots, \alpha_L}$. For the norms the order of these coefficients does not matter. The 1-norm is then given by $\|A\|_1 = \sum_{\{\alpha\}} |a_{\alpha_1, \dots, \alpha_L}|$. In symbolic calculations, where operators are obtained in the form (II.5), this means that we simply have to sum up the absolute values, or the absolute values squared, of the operator A written in the local basis $\{\sigma_i^\alpha\}$.

The two matrix norms which we have defined in Eq. (II.4) are sub-additive and the 1-norm is an upper bound for the 2-norm

$$\begin{aligned} \|A + B\|_p &\leq \|A\|_p + \|B\|_p \\ \|A\|_2 &\leq \|A\|_1. \end{aligned} \quad (\text{II.6})$$

However, due to the rescaling by the factor $(\text{tr } \mathbb{1}_{M \times M})^{-1/2}$ the two norms are no longer sub-multiplicative. We note, however, that if $A = J_A \sigma_1^{\alpha_1} \otimes \dots \otimes \sigma_L^{\alpha_L}$ and $B = J_B \sigma_1^{\beta_1} \otimes \dots \otimes \sigma_L^{\beta_L}$, i.e., both operators have only one coefficient in Eq. (II.5) which is non-zero, then

$$\|AB\|_p = \|A\|_p \|B\|_p = |J_A| |J_B|. \quad (\text{II.7})$$

While the 2-norm (Hilbert-Schmidt norm) is physically more relevant because it is induced by the standard scalar product in quantum mechanics, the 1-norm is often easier to calculate and provides an upper bound for the 2-norm.

A. General Case

The case of the Euclidean norm growth for a one-dimensional nearest-neighbor model without any further restrictions on the form of the nearest-neighbor Hamiltonian has been considered in Ref. [30]. Here we briefly recapitulate the derivation of the general bound to contrast it with the tighter bounds which we derive below in the special cases of free-fermion and localized models.

Let us define $H = \sum_I \sum_{a=1}^C h_I^a$ where h_I^a are local Hamiltonian densities of the form $h_I^a = J_I^a \sigma_I^{\alpha_1} \otimes \sigma_{I+1}^{\alpha_2}$. We note that the commutator (II.1) is zero if the local operator A and the local Hamiltonian densities h_I^a do not form a connected cluster. Let $\{I_1, \dots, I_k\}$ be a set of points which fulfills the adjacency condition, then

$$\begin{aligned} \| [H, A]^{(k)} \| &= \| \sum_{\{I_1, \dots, I_k\}} \sum_{\{a_I\}} [h_{I_1}^{a_{I_1}}, [h_{I_2}^{a_{I_2}}, \dots, [h_{I_k}^{a_{I_k}}, A]]] \| \\ &\leq \sum_{\{I_1, \dots, I_k\}} \sum_{\{a_I\}} \| [h_{I_1}^{a_{I_1}}, [h_{I_2}^{a_{I_2}}, \dots, [h_{I_k}^{a_{I_k}}, A]]] \| \end{aligned} \quad (\text{II.8})$$

where we have used the sub-additivity property (II.6). The commutator now is determined by terms which are products of single operators in the $\{\sigma_i^\alpha\}$ basis and we can use Eq. (II.7) implying that

$$\| h_{I_1}^{a_{I_1}} h_{I_2}^{a_{I_2}} \dots h_{I_k}^{a_{I_k}} A \| = \| h_{I_1}^{a_{I_1}} \| \| h_{I_2}^{a_{I_2}} \| \dots \| h_{I_k}^{a_{I_k}} \| \| A \| . \quad (\text{II.9})$$

There are 2^k terms of this kind and we therefore find

$$\begin{aligned} \| [H, A]^{(k)} \| &\leq 2^k \sum_{\{I_1, \dots, I_k\}} \sum_{\{a_I\}} \underbrace{\| h \| \dots \| h \|}_{k\text{-many}} \| A \| \\ &\leq (2CJ)^k \| A \| \sum_{\{I_1, \dots, I_k\}} \end{aligned} \quad (\text{II.10})$$

where we have used that $\| h_I^a \| = J_I^a \leq J = \max_{I,a} \{J_I^a\}$ and $\sum_{\{a_I\}} = C^k$.

Eq. (II.10) is now a purely combinatorial problem. We need to figure out how many different arrangements of the lattice points $\{I_1, \dots, I_k\}$ exist such that a connected cluster is formed. Without repeated indices, j local adjacent Hamiltonians form a cluster with j bonds. At each step, one can either attach a local Hamiltonian to the right or to the left of the existing cluster. Thus, as for the random walk in one dimension, there are 2^j possibilities to form a cluster with j bonds. Lastly, consider the case that we have a cluster of length j and $k \geq j$ local Hamiltonians h_I . Then the question is how many ways there are to ‘distribute’ those local Hamiltonians on the j bonds of the cluster. This is the same question as asking how many ways there are to partition k elements into j non-empty sets. The answer is given by the Stirling numbers of the second kind, $S(k, j)$. We therefore obtain

$$\sum_{\{I_1, \dots, I_k\}} = \sum_{j=1}^k 2^j S(k, j) = B_k(2) \quad (\text{II.11})$$

where $B_k(x)$ is the Bell (Touchard) polynomial. The general bound is therefore given by

$$s^{(p)}(k) \equiv \| [H, A]^{(k)} \|_p \leq \| A \|_p (2CJ)^k B_k(2) \quad (\text{II.12})$$

where $p = 1, 2$ is the 1-norm or the 2-norm defined earlier. We note that this bound is also valid for any sub-multiplicative norm.

We are, in particular, interested in the asymptotic growth of the operator norm for large k . In this limit, the Bell polynomial scales as

$$B_k(2) \sim \frac{\exp[-k(1 + \ln W(k/2) - W^{-1}(k/2))]}{\sqrt{W(k/2) + 1}} e^{-2k} \quad (\text{II.13})$$

where $W(x)$ is the Lambert W function [39]. Using the Stirling formula $k^k \sim k! \exp(k) / \sqrt{2\pi k}$ we can rewrite the asymptotics as

$$\begin{aligned} B_k(2) &\sim \frac{e^{-2k}}{\sqrt{2\pi k (W(k/2) + 1)}} \\ &\times \exp \left[k \frac{1 - W(k/2) \ln W(k/2)}{W(k/2)} \right]. \end{aligned} \quad (\text{II.14})$$

This means that the bound (II.12) grows faster than exponentially and almost factorially. We note that the term in the exponential in the second line of (II.14) only becomes negative for $k \gtrsim 20$ thus suppressing the initial almost factorial growth. For large k , one can also use that $W(k) \sim \ln k - \ln \ln k$ to see from Eq. (II.13) that $B_k(2) \sim (k/\ln k)^k$.

We can also ask the question how many *distinct* terms are possible in the commutator $[H, A]^{(k)}$. Note that this question is different from the question of how many connected clusters exist which we addressed above because connected clusters formed in different ways can result in the same operator. Let us assume that our system has a basis of $f - 1$ local operators plus the local identity \mathbb{I}_j . At order k , clusters have at most length $k + 1$ and, if the operator A was placed on site $j = 0$, extend from sites $-k, -k + 1, \dots, 0$ to the right. I.e., there are $k + 1$ clusters of length $k + 1$ with each shifted by one lattice site to the right compared to the previous one. For the cluster starting at $-k$, we can put any of the $f - 1$ local operators or the identity on each of the $k + 1$ sites leading to f^{k+1} possible operators. For the cluster starting at site $-k + 1$, we have to put one of the $f - 1$ local operators at the right most site, $j = 1$, to obtain operators distinct from the ones already constructed. Thus, this cluster will add $(f - 1)f^k$ possible operators. The same construction also works for the remaining $k - 1$ clusters. We can therefore bound the total number of possible distinct operators occurring in the commutator $[H, A]^{(k)}$ by

$$n(k) \leq f^{k+1} + k(f - 1)f^k = (kf - k + f)f^k. \quad (\text{II.15})$$

For a generic system, we thus expect that the number of distinct terms $n(k)$ in the commutator grows exponentially. As we will discuss in more detail below, the terms occurring in the commutator can be represented as nodes in a graph and $n(k)$ is directly related to the complexity of this graph.

To summarize, if a system does not have *local* operators which are conserved, then the hypothesis is that the bound on the total norm (II.12) is asymptotically tight [30]. Importantly, a norm growth $s(k) \sim (k/\ln k)^k$ is not possible in regular graphs or Cayley trees where the norm cannot grow faster than exponential. Many-body systems and the question of localization in such systems are therefore qualitatively different from studies of localization on regular graphs [40, 41]. Next, we consider non-interacting systems which are one example of systems corresponding to regular graphs where stricter, exponential bounds on the norm can be derived.

B. Free Fermions

The main difference between a general, interacting system and a free-fermion system is that in the latter case the commutator of a one-body operator with the Hamiltonian always remains a one-body operator. Therefore many of the connected clusters leading to the the bound

(II.11) do not contribute. Here, a free-fermion model is a system with a bilinear Hamiltonian of the form $H = \sum_{j,k} h_{jk} c_j^\dagger c_k$ where $c_j^{(\dagger)}$ is a fermionic annihilation (creation) operator at site j . We do not include pair creation and annihilation terms in H but note that the arguments in the following remain valid qualitatively if they are included.

Our starting point to prove a bound in the free-fermion case is the last line of Eq. (II.10). We now want to understand how many distinct connected clusters there are which give a non-zero contribution to the sum. The Hamiltonian in this case is, in general, a sum of C one-body terms, $H = \sum_I \sum_{a=1}^C h_I^a$ such as nearest-neighbor hoppings and local potentials. Now consider a connected cluster $\{I\} = \{I_1, \dots, I_k\}$ which gives a non-zero contribution to the sum in Eq. (II.10). Since the commutator $[H, A]^{(k)}$ is always a one-body operator if A is a one-body operator, there is one fermionic operator on a site i and another fermionic operator on a site j for each such cluster. Then, growing the cluster the only contributions which can potentially be non-zero will come from adding a one-body term h^a on one of the bonds $I_{i-1}, I_i, I_j, I_{j+1}$. I.e., there are at most 4 possibilities to build a new non-zero cluster with $k + 1$ elements. While this is, in general, overcounting the number of possibilities we can thus iteratively show that

$$\sum_{\{I_1, \dots, I_k\}} \leq 4^k \quad (\text{II.16})$$

resulting in the bound

$$\| [H, A]^{(k)} \| \leq \| A \| (8CJ)^k. \quad (\text{II.17})$$

For a free-fermion system, the operator norm growth is thus at most exponential [42].

We can also again consider the question how many distinct terms can at most occur in the commutator $[H, A]^{(k)}$. As in the general case, the clusters have length of at most $k + 1$ and have $k + 1$ different starting points (leftmost lattice site in the cluster). The difference is that we now have to distribute only two operators, a fermionic creation operator c_i^\dagger and a fermionic annihilation operator c_j , over the cluster. For the first cluster, we have $(k + 1)$ possibilities to place the creation and $(k + 1)$ possibilities to place the annihilation operator for a total of $(k + 1)^2$ possible distinct terms. For the other clusters, we have to place either c^\dagger or c on the rightmost site to get new distinct terms. The other operator can then be placed on any of the $k + 1$ sites for a total of $2(k + 1) - 1 = 2k + 1$ (placing both operators on the rightmost site results in only one new term) distinct new terms for each of the k remaining clusters. A bound for the total number of distinct terms is thus given by

$$n(k) \leq (k + 1)^2 + k(2k + 1) = 3k(k + 1) + 1. \quad (\text{II.18})$$

In a free-fermion system, the number of distinct operators in the commutator $[H, A]^{(k)}$ thus grows quadratically

with the order of the commutator k . As we will show below when considering the example of the XX chain, the quadratic growth of the number of distinct operators is directly related to a regular structure of the corresponding graph with a constant number of nodes and edges at each level.

C. Localization

In a localized phase, a local operator A is expected to remain localized to a finite region of space of length ξ_{loc} (up to exponentially small tails) when commuted k -times with the Hamiltonian. This means that we expect that connected clusters of length $j \gg \xi_{\text{loc}}$ give almost no contribution to the norm. Neglecting such clusters leads to

$$\sum'_{\{I_1, \dots, I_k\}} = \sum_{j=1}^{\min(k, \xi_{\text{loc}})} 2^j S(k, j). \quad (\text{II.19})$$

Asymptotically, for large k , we thus obtain

$$\sum_{j=1}^{\xi_{\text{loc}}} 2^j S(k, j) \sim \sum_{j=1}^{\xi_{\text{loc}}} \frac{2^j j^k}{k!} < \frac{2^{\xi_{\text{loc}}}}{(\lceil \xi_{\text{loc}} \rceil - 1)!} \xi_{\text{loc}}^k \quad (\text{II.20})$$

where we have used the asymptotic scaling $S(k, j) \sim j^k / j!$ of the Stirling numbers of the second kind for $k \gg j$. The operator growth in a localized phase is therefore at most exponential

$$\| [H, A]^{(k)} \| \leq \| A \| \frac{2^{\xi_{\text{loc}}}}{(\lceil \xi_{\text{loc}} \rceil - 1)!} (2\xi_{\text{loc}} C J)^k. \quad (\text{II.21})$$

In deriving this bound, we have made the simplifying assumption that the contributions of all clusters with lengths $j \gg \xi_{\text{loc}}$ can be neglected. Given that with increasing length also more possibilities exist to distribute the local Hamiltonians h_I^a , one might worry that this assumption is not justified. We will show in App. A that the argument remains valid if clusters with $j > \xi_{\text{loc}}$ are included.

We note that both the free-fermion case and the localized case show an exponential growth of the operator norm. Thus, the total operator norm is insufficient to distinguish a non-localized free-fermion phase from a localized interacting or non-interacting phase. The total norm, however, does tell us whether or not a system is ergodic. What does distinguish non-ergodic non-localized from localized phases though is how different terms in the commutator contribute to the norm. If we denote by $[H, A]_l^{(k)}$ the terms in the commutator of order k which have support on l lattice sites, then we expect that in the localized case

$$s_l^{(p)}(k) \equiv \| [H, A]_l^{(k)} \|_p \sim e^k e^{-l}. \quad (\text{II.22})$$

For a non-localized phase, on the other hand, the initially local operator A will spread over the entire lattice, implying that terms in the commutator with $l \ll k$ should contribute approximately equally to the total norm.

To summarize, the operator growth hypothesis is that the bound (II.12) is asymptotically tight for an ergodic system which thus should have an operator norm $s(k)$ which grows faster than exponential with the order of the commutator k . In an interacting localized phase—the putative many-body localized phase—the norm growth, as we have proven, can instead only be at most exponential. For a free-fermion model, the norm growth is also always at most exponential whether it is in a localized phase or not. In the latter case, we can distinguish a localized from a non-localized phase by studying the contributions $s_l(k)$ from terms which are supported on l lattice sites to the total norm of the commutator $s(k)$.

III. THE XXZ MODEL WITH (QUASI-)RANDOM FIELDS

As a specific example, we want to consider the XXZ chain with random or quasi-random magnetic fields

$$H = \sum_j (\sigma_j^x \sigma_{j+1}^x + \sigma_j^y \sigma_{j+1}^y + \Delta \sigma_j^z \sigma_{j+1}^z + 2h_j \sigma_j^z). \quad (\text{III.1})$$

Here, $\sigma^{x,y,z}$ are Pauli spin-1/2 matrices, Δ characterizes the spin exchange anisotropy, and h_j are magnetic fields. As the operator which we will commute with the Hamiltonian H we consider a single local σ_j^z . The model (III.1) is equivalent to a spinless fermion model using the Jordan-Wigner transformation

$$\begin{aligned} \sigma_j^+ &= S_j c_j^\dagger, & \sigma_j^- &= S_j^\dagger c_j, & \sigma_j^z &= 2c_j^\dagger c_j - 1, \\ S_j &= \exp \left[-i\pi \sum_{k=1}^{j-1} c_k^\dagger c_k \right] = \prod_{k=1}^{j-1} \left[1 - 2c_k^\dagger c_k \right] \end{aligned} \quad (\text{III.2})$$

with $\sigma_j^\pm = (\sigma_j^x \pm i\sigma_j^y)/2$ leading to

$$\begin{aligned} \frac{H}{4} &= \frac{1}{2} \sum_j \left\{ c_j^\dagger c_{j+1} + c_{j+1}^\dagger c_j \right\} \\ &+ \sum_j \left\{ \Delta(n_j - 1/2)(n_{j+1} - 1/2) + h_j(n_j - 1/2) \right\}. \end{aligned} \quad (\text{III.3})$$

Here $c_j^{(\dagger)}$ are fermionic annihilation (creation) operators and $n_j = c_j^\dagger c_j$. In the following, we will investigate the non-interacting case, $\Delta = 0$, and the interacting, isotropic Heisenberg case, $\Delta = 1$.

A. Non-interacting case

We will first concentrate on the non-interacting free-fermion case, $\Delta = 0$, where localization is well understood. Here we want to show that the general bounds

for the total norm of the k -th order commutator derived earlier do apply and that we can distinguish localized from non-localized phases by resolving the contributions to the norm by the length of the spatial support of each term in the commutator.

1. No disorder

The first specific case we will consider is the free-fermion case, $\Delta = 0$, without any magnetic fields, $h_j = 0$. In this case, the entire structure of the commutator $[H, \sigma_0^z]^{(k)}$ can be worked out analytically. We find these results instructive and will discuss them in detail here to motivate a description of the commutator by graphs where the vertices are the terms generated and the edges denote their contribution to the 1-norm.

The full analytical solution is best understood in the fermionic language: the commutator $[H, c_0^\dagger c_0]^{(k)}$ will only contain terms which are one-particle operators, i.e., terms which contain exactly one annihilation and one creation operator. More specifically, we find for the case that the order of the commutator k is odd that

$$\begin{aligned} [H, \sigma_0^z]^{(k)} &= \sum_{l=0}^{\frac{k-1}{2}} \sum_{s=-\frac{k+1}{2}-l}^{\frac{k-1}{2}-l} a_{kls} \left\{ \sigma_s^x \bigotimes_{j=s+1}^{s+2l} \sigma_j^z \sigma_{s+2l+1}^y \right. \\ &\quad \left. - \sigma_s^y \bigotimes_{j=s+1}^{s+2l} \sigma_j^z \sigma_{s+2l+1}^x \right\} \quad (\text{III.4}) \\ &= -\frac{2}{i} \sum_{l=0}^{\frac{k-1}{2}} \sum_{s=-\frac{k+1}{2}-l}^{\frac{k-1}{2}-l} a_{kls} \{ c_s^\dagger c_{s+2l+1} - h.c. \} \end{aligned}$$

with coefficients a_{kls} which are discussed below. For k even, we find instead

$$\begin{aligned} [H, \sigma_0^z]^{(k)} &= \sum_{s=-\frac{k}{2}}^{\frac{k}{2}} a_{k0s} \sigma_s^z \\ &\quad + \sum_{l=1}^{\frac{k}{2}} \sum_{s=-\frac{k}{2}-l}^{\frac{k}{2}-l} a_{kls} \left\{ \sigma_s^x \bigotimes_{j=s+1}^{s+2l-1} \sigma_j^z \sigma_{s+2l}^x \right. \\ &\quad \left. + \sigma_s^y \bigotimes_{j=s+1}^{s+2l-1} \sigma_j^z \sigma_{s+2l}^y \right\} \quad (\text{III.5}) \\ &= 2 \sum_{s=-\frac{k}{2}}^{\frac{k}{2}} a_{k0s} (n_s - 1/2) \\ &\quad - 2 \sum_{l=1}^{\frac{k}{2}} \sum_{s=-\frac{k}{2}-l}^{\frac{k}{2}-l} a_{kls} \{ c_s^\dagger c_{s+2l} + h.c. \}. \end{aligned}$$

Note that the commutator has the form of a current density for k odd and that of a charge density for k even.

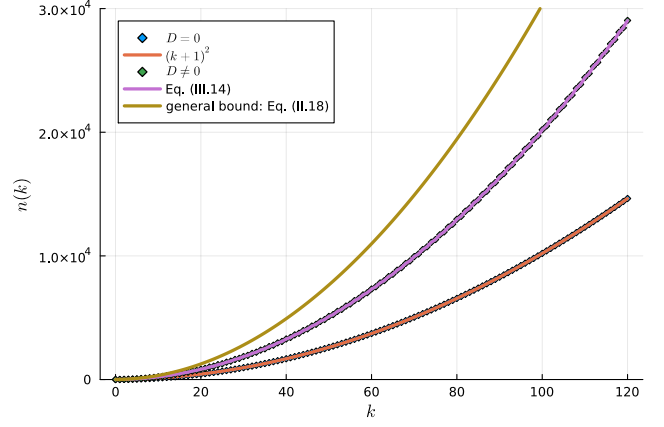


FIG. 1. XX model: Without disorder, the number of distinct terms $n(k)$ in $[H, \sigma_0^z]^{(k)}$ grows as $(k+1)^2$ while it grows according to Eq. (III.14) with disorder. The general bound (II.18), valid for any free-fermion model, is also shown.

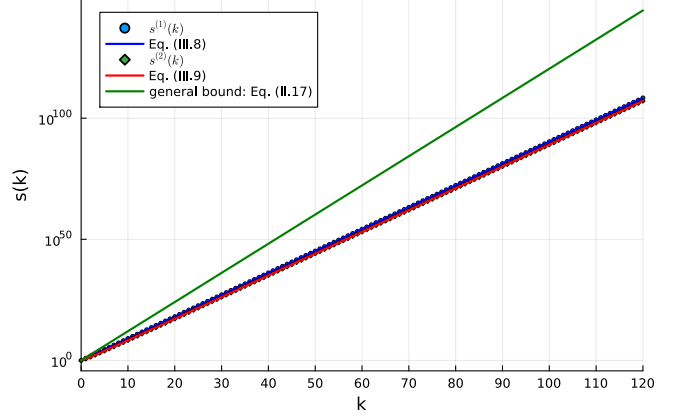


FIG. 2. In the XX model without disorder the norms grow as $s^{(1)}(k) = 8^k$ and $s^{(2)}(k) = 2^k \binom{2k}{k}$. Note that on this scale both results are very close to each other. The 2-norm is only slightly smaller than the 1-norm. Also shown is the general bound, Eq. (II.17), with $C = 2$.

From the formulas (III.4) and (III.5) we can immediately read off that there are $n(k) = \frac{k+1}{2}(k+1) \cdot 2 = k+1 + \frac{k}{2}(k+1) \cdot 2 = (k+1)^2$ different terms generated at order k , both in the odd and in the even case. We confirm this result by calculating the commutator using symbolic manipulations up to high order, see Fig. 1. We want to stress that the quadratic growth of the number of terms is a special property of a free fermionic model where a one-body operator, when commuted with the Hamiltonian, always remains a one-body operator. What changes is only the separation between the creation and annihilation operator (support of the one-body operator) and the number of different sites where the first of the fermionic operators is located. Both the allowed separations as well as the possible sites for the first fermionic operator grow linearly in k , leading to the overall quadratic growth in

the number of distinct terms in the commutator. We already want to note here that this behavior is expected to change dramatically in the interacting case.

In the simple, non-disordered XX case considered here, we can even take it one step further and calculate the coefficients a_{kls} exactly. These coefficients are completely determined by the coefficient matrices C_k which are defined by

$$(C_k)_{ij} = 2^k \binom{k}{i-1} \binom{k}{j-1} \quad (\text{III.6})$$

with $1 \leq i, j \leq k+1$. In the following, we concentrate on the case of k odd which has a slightly simpler structure, see Eq. (III.4). In this case we find, in particular, that

$$a_{kls} = i(-1)^s (C_k)_{s+\frac{k+3}{2}+l, \frac{k+1}{2}-l}. \quad (\text{III.7})$$

From the result (III.7) we can now determine the total norms of the commutator and, furthermore, we can even determine which operators contribute how much to the total norm. From Eq. (III.4) and Eq. (III.7) we find that the set of the coefficients $\{|a_{kls}|\}$ is the same as $\{(C_k)_{ij}\}^2$, i.e., each entry in C_k appears two times. We therefore find

$$s^{(1)}(k) \equiv \| [H, \sigma_0^z]^{(k)} \|_1 = 2 \sum_{i=1}^{k+1} \sum_{j=1}^{\frac{k+1}{2}} (C_k)_{ij} = 8^k \quad (\text{III.8})$$

where we have used the explicit form of the coefficient matrix (III.6). Similarly, we find

$$(s^{(2)}(k))^2 \equiv \| [H, \sigma_0^z]^{(k)} \|_2^2 = 2 \sum_{i=1}^{k+1} \sum_{j=1}^{\frac{k+1}{2}} (C_k)_{ij}^2 = 2^{2k} \binom{2k}{k}^2. \quad (\text{III.9})$$

Asymptotically, the 2-norm therefore grows as

$$s^{(2)}(k) = 2^k \binom{2k}{k} \approx \frac{8^k}{\sqrt{\pi k}} \quad (\text{III.10})$$

where we have used Stirling's formula. This shows that the 2-norm grows also exponentially in k but with a correction which makes it always smaller than the 1-norm as expected on general grounds, see Eq. (II.6). We can again check these results for finite k by symbolic manipulations, see Fig. 2.

Finally, we can study how much terms which extend over a distance l contribute to the total norm. We consider the case k odd where the amplitude a_{kls} for terms which have support on $2l+2$ sites is given by Eq. (III.7). We find again that the same entries appear multiple times and that all prefactors for a given l are represented by the column $j = \frac{k+1}{2} - l$ of the coefficient matrix $(C_k)_{ij}$. Summing over all initial sites we thus obtain

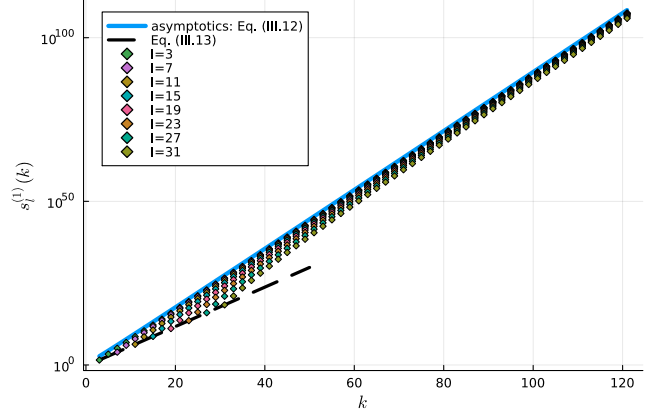


FIG. 3. For $k \gg l$ the norm of operators with support on l sites is asymptotically described by Eq. (III.12) and is independent of l . The exact value (III.13) when $s_l^{(1)}(k)$ first becomes non-zero is also shown.

$$\begin{aligned} s_{2l+2}^{(1)}(k) &= \| [H, \sigma_0^z]_{2l+2}^{(k)} \|_1 = \sum_i |a_{kli}| \quad (\text{III.11}) \\ &= 2 \sum_{i=1}^{k+1} (C_k)_{i, \frac{k+1}{2}-l} = 2^{2k+1} \binom{k}{\frac{k-1}{2}-l} \\ &\rightarrow s_l^{(1)}(k) = 2^{2k+1} \binom{k}{\frac{k+1-l}{2}} \end{aligned}$$

where in the last line we transformed the equation to show the support on l sites rather than on $2l+2$ sites. In the limit $k \gg l$ we can apply Stirling's formula and find

$$s_l^{(1)}(k) \approx \sqrt{\frac{8}{k\pi}} 8^k. \quad (\text{III.12})$$

This means that all the terms *contribute equally independently of the length of their support* l which clearly indicates delocalization. We also note that the largest possible support at commutator order $k-1$ are k sites with

$$s_k^{(1)}(k-1) = 2^{2k-1}. \quad (\text{III.13})$$

These analytical results can be checked by symbolic manipulations, see Fig. 3.

While we have been able to exactly calculate the k -th order commutator in the non-interacting, non-disordered case, see Eqs. (III.4, III.5, III.7), this is clearly no longer possible, even in principle, if random fields are included. On a positive note, this is also more than what we need. To distinguish between free-fermionic localized and non-localized phases and interacting localized and non-localized phases it is sufficient to consider the total commutator norm and the norm of the terms in the commutator which are supported on l sites. This can be achieved more efficiently by developing graphs where the vertices represent the possible terms at order k and the edges represent the contribution to the 1-norm. Fig. 4 shows such a graph for the non-interacting model. The case without

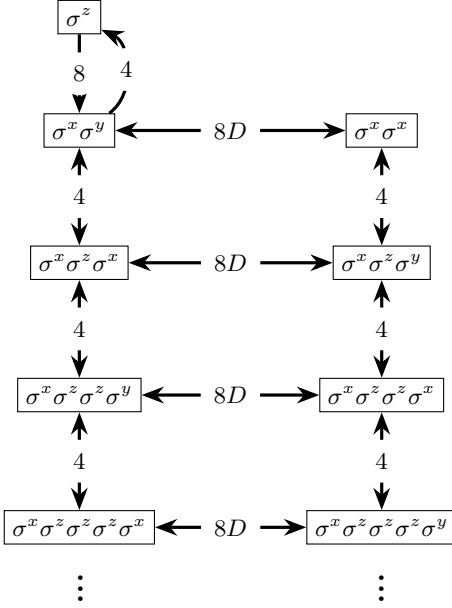


FIG. 4. Graph for the commutator $[H, \sigma_0^z]^{(k)}$ in the non-interacting case, $\Delta = 0$. The vertices represent the possible terms with support on l sites ($l = 1, 2, \dots$ from top to bottom) while the edges represent the contribution to the 1-norm. The number of traversed edges equals the order of the commutator k . Terms obtained by $\sigma^x \leftrightarrow \sigma^y$ are grouped together into a single vertex. Without disorder, $D = 0$, only the terms in the left column will be present.

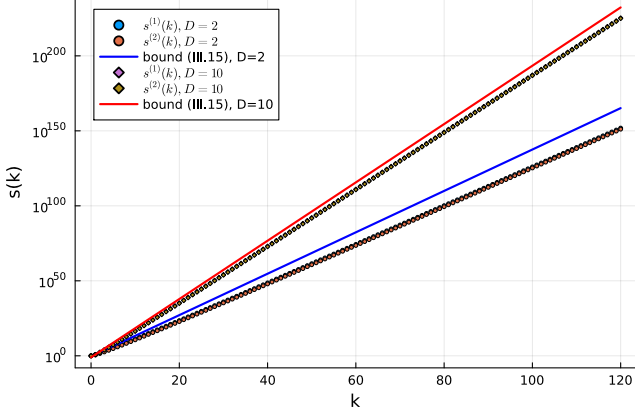


FIG. 5. $s^{(1)}(k)$ and $s^{(2)}(k)$ for the Anderson model with $D = 2$ and $D = 10$. The results are averaged over 100 samples. Note that the 2-norm is only slightly smaller than the 1-norm and the two norms are almost indistinguishable on this scale. The bound (III.15) is shown as well.

random magnetic fields discussed here corresponds to the case $D = 0$ where only the terms in the left column are present. In this case, the graph is a 2-regular graph with one node per level and 2 edges per node. The constant number of nodes per level is directly reflected in the quadratic growth of the number of distinct terms $n(k)$.

To obtain $s^{(1)}(k)$, we have to sum over all weighted

walks through the graph which start at the top and have length k by multiplying the values of all traversed edges, irrespective of the vertex the walk ends on. If, on the other hand, we want to calculate only the contributions of terms which have support on l sites, $s_l^{(1)}(k)$, then we have to sum only over those weighted walks with k steps which end at a vertex with terms on l sites. We discuss this approach to calculating or bounding the norm of the commutator in more detail in App. D. Fig. 4 also already shows how the graph has to be modified in the Anderson case which we discuss next.

2. Anderson Localization

Next, we consider the case of quenched disorder where the magnetic fields h_j in the Hamiltonian (III.1) are drawn randomly from a box distribution, $h_j \in [-D, D]$. We note that in the one-dimensional case considered here any amount of disorder is a relevant perturbation. The model is localized for all $D > 0$. Since h_j is random, we cannot expect exact results for the norm. Instead, we will derive strict upper bounds.

What we can do exactly, however, is to count the number of distinct terms $n(k)$ in the commutator which occur at order k and which is independent of the specific disorder realization. This is easiest done by making use of the graph, see Fig. 4, and by taking also into account the different possibilities where in the lattice these terms can be located. Doing so we find

$$n(k) = 2k(k+1) + \begin{cases} 1 & \text{even} \\ 1-k & \text{odd} \end{cases} \quad (\text{III.14})$$

This result is compared to symbolic calculations in Fig. 1. We stress once more that Eq. (III.14) is independent of the type of disorder or the specific disorder configuration and is thus also valid in the Aubry-André case discussed in Sec. III A 3. Note that while the precise number of terms has changed as compared to the non-disordered case, importantly the number of terms still only increases quadratically with k .

To bound the 1-norm, we use the graph shown in Fig. 4. With random fields, the additional terms in the right column and the corresponding additional paths are present. In the first step, we collect a factor of 8 in the 1-norm. In every other step, we can collect at most a factor $8 + 8D$ where we have bounded the disorder by $|h_j| \leq D$. We therefore obtain the following bound

$$s^{(1)}(k) \leq 8(8 + 8D)^{k-1} = 8^k(D+1)^{k-1}. \quad (\text{III.15})$$

As expected, we find that the norm has an exponential bound. Note that this bound increases with increasing disorder D , see Fig. 5. Also note that for $D = 0$ we obtain the exact result for the norm in the non-disordered case, Eq. (III.8). Apart from the initial node and the node on the top right, the graph with disorder is a 3-regular graph. I.e., each node is connected to three edges. We

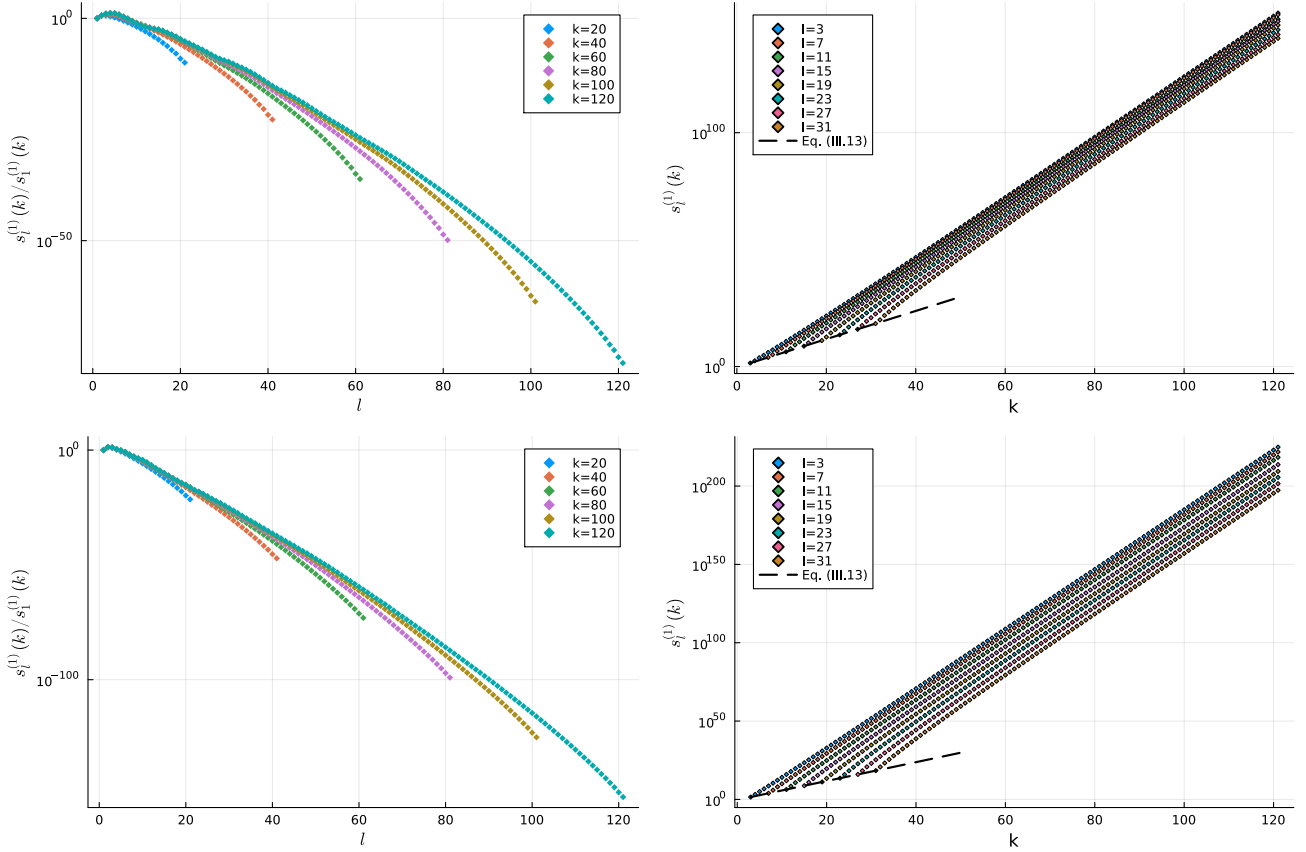


FIG. 6. Left column: Norm ratio $s_l^{(1)}(k)/s_1^{(1)}(k)$ for a fixed k as a function of l for the Anderson model with $D = 2$ (top row) and $D = 10$ (bottom row). Right column: $s_l^{(1)}(k)$ for a fixed l as a function of k . The data are averaged over 100 samples. Note that the value of $s_l^{(1)}(k)$ when it first becomes non-zero at $k = l - 1$ is not affected by disorder, see Eq. (III.13).

note that in every n -regular graph the norm $s^{(1)}(k)$ can not grow faster than exponential. This remains true even if the number of nodes increases with k as, for example, in a Cayley tree as long as the number of edges per node is constant. This follows immediately from the fact that $s^{(1)}(k)$ is the sum of the product of edge values along all possible paths of length k . That $n(k)$ grows only quadratically means that the graph in the free-fermion case is particularly simple and has a constant number of nodes at each level.

To see the difference between a free-fermionic model, where an initially localized operator spreads over the entire chain, and a system where the operator remains localized it is thus not sufficient to study the total operator norm. Instead, we have to investigate the spatial structure of the terms in the commutator at order k . Based on the graph in Fig. 4, we can derive a bound for the contribution of terms with support on l sites to the norm at order k . We use again that $|h_j| \leq D$. The derivation of this bound is discussed in detail in App. D 2. Here, we will consider the simplest possible approach where we only consider those terms with support on l sites which have the largest possible number of factors h_j . This approach is justified for $D \gg 1$ and, as we will argue, gives

the same asymptotics in the limit $k \gg l \gg 1$ as the more sophisticated approach discussed in App. D 2. Let us first consider terms which have support on a single site, i.e., which are of the form σ_j^z . As is obvious from the graph in Fig. 4, such terms are only generated at even orders of k . We collect the largest number of factors h_j if we go down one level, then travel $k - 2$ times along the vertical direction, and then go back up to the top of the graph. The 1-norm of such terms is thus bounded by

$$s_1^{(1)}(k) \leq 8 \times (8D)^{k-2} \times 4 = 2^{2k+1}(2D)^{k-2}. \quad (\text{III.16})$$

Next, we consider the norm of terms with support on $l \geq 2$ sites with the largest number of possible h_j factors. In the first step, we have to go one level down in the graph in Fig. 4 which contributes a factor of 8. To get to terms with support on $l \geq 2$ sites we have to take another $l - 2$ steps down, contributing a factor 4^{l-2} . We can distribute these steps among a total of $k - 1$ remaining steps, i.e., there are $\binom{k-1}{l-2}$ possibilities. Finally, we get a factor $(8D)^{k-1-(l-2)}$ from the remaining steps along the vertical lines in the graph. Thus, the one norm of such terms is bounded by

$$s_l^{(1)}(k) \leq \binom{k-1}{l-2} 2^{2k+1} (2D)^{k-l+1}. \quad (\text{III.17})$$

The relative contribution to the norm of terms with support on l sites when normalized to the contribution coming from single-site operators is thus given by

$$\frac{s_l(k)}{s_1(k)} \lesssim \binom{k-1}{l-2} (2D)^{3-l} \approx \frac{1}{\sqrt{2\pi l}} \left(\frac{ke}{l}\right)^l e^{-\frac{l^2}{2k}} (2D)^{3-l}. \quad (\text{III.18})$$

We note that while for a fixed k we indeed find that the ratio (III.18) goes exponentially to zero for large l , there is a maximum in the ratio which shifts to larger l with increasing k . This is not quite the behavior we expect. Instead, we expect that with increasing k the ratio (III.18) converges to a function which is exponentially decreasing in l . Here it is important to note that (III.18) is only an upper bound. In particular, we have only considered those paths which have a maximum number of h_j factors. There are, however, many additional paths and we expect that the prefactor in (III.18) will eventually converge with k for a given l . This is consistent with what we observe from symbolic manipulations to finite orders of k , see Fig. 6. We note that in contrast to the non-disordered case where $s_l(k)$ grows exponentially and independent of l for $k \gg l$, see Eq. (III.12) and Fig. 3, we find that with quenched disorder

$$s_l(k) \sim e^k D^{-l}, \quad (\text{III.19})$$

see Fig. 7. The spatial structure of the norm contributions $s_l(k)$ thus provide a clear distinction between the non-localized and localized phases.

3. Aubry-André model

To further check that the exponential decay of $s_l(k) = \|[H, \sigma_0^z]_l^{(k)}\|$ with l is indeed the signature of a localized system, we consider the Aubry-André model next. This is a model which is typically formulated as a fermionic model (III.3) where instead of quenched disorder we have a periodic potential

$$h_j = \frac{\lambda}{2} \cos(2\pi\beta j + \phi). \quad (\text{III.20})$$

Then, for β Diophantine and almost any ϕ —excluding a set of measure zero of resonant phases—the eigenstates of the Aubry-André model are localized for $\lambda > 2$ [43, 44]. A common choice is to use the golden ratio $\beta = (1 + \sqrt{5})/2$. The model thus provides an important test case where both a non-localized and a localized phase exist. Below the transition in the non-localized phase we expect that $s_l(k)$ is qualitatively described by Eq. (III.12), i.e., grows with k independent of l for $k \gg l$. In the localized phase, on the other hand, we expect that $s_l(k)$ is exponentially localized, see Eq. (III.19). Note that the graph for the Aubry-André model is the same as the one

in the Anderson case shown in Fig. 4 with $D \rightarrow \lambda/2$ on the edges. With this replacement, also the bound (III.15) holds. We note that the considerations which let us to Eq. (III.19) in the Anderson case were valid only in the case of strong disorder. In this limit, they remain valid for the Aubry-André model. That the exponential decaying structure for the spatial support of the norm remains unchanged for all $D \neq 0$ in the Anderson case while there is a transition to the structure (III.12), which is independent of l for $k \gg l$, for the Aubry-André model is beyond the strong disorder arguments we used in the previous section. All these results and expectations outlined above are fully consistent with the symbolic computations shown in Fig. 8. Note that the data in the left panels for the non-localized phase are shown on a linear scale while the results in the right panels for the localized phase are shown on a logarithmic scale.

While other methods might be better suited to determine the exact phase transition point, there is a clear *qualitative* difference in the scaling of $s_l(k)$ between the extended and the localized phase. The operator growth $s_l(k)$ therefore allows for an unambiguous distinction between these two phases.

B. Interacting case

With the results we have established in the non-interacting non-localized and localized cases, we can now look at the interacting isotropic Heisenberg (XXX) model, i.e., the Hamiltonian (III.1) with $\Delta = 1$. A fundamental general difference in interacting as compared to non-interacting models is that one-body operators do not remain one-body operators when commuted with the Hamiltonian. This leads to a qualitatively different phenomenology in the operator growth with exponentially many more terms and paths.

We also note that the Heisenberg model without disorder is a so-called integrable model which has, what is commonly called, an infinite set of local conserved charges O with $[H, O] = 0$ in the thermodynamic limit. It is crucial to note though that ‘local’ is meant here in an entirely different way. These charges are in no way localized but rather can be written as $O = \sum_j o_j$ where o_j is a local density acting on a finite number of lattice sites. I.e., the charge densities are local but the entire conserved operator O is not and rather acts on the entire lattice. The trivial examples are the Hamiltonian itself, $H = \sum_I h_I$ and the magnetization $M = \sum_I \sigma_I^z$. What is special about integrable models is that an infinite set of operators of this type exist which allows to uniquely characterize all eigenstates by the corresponding quantum numbers. The eigenspectrum of the model can thus be calculated exactly by using the Bethe ansatz [45, 46]. For the question of *local operator growth*, integrability is not relevant and we do not expect to see any difference to a non-integrable model. Even if we break integrability, the magnetization M is still conserved as long as $U(1)$

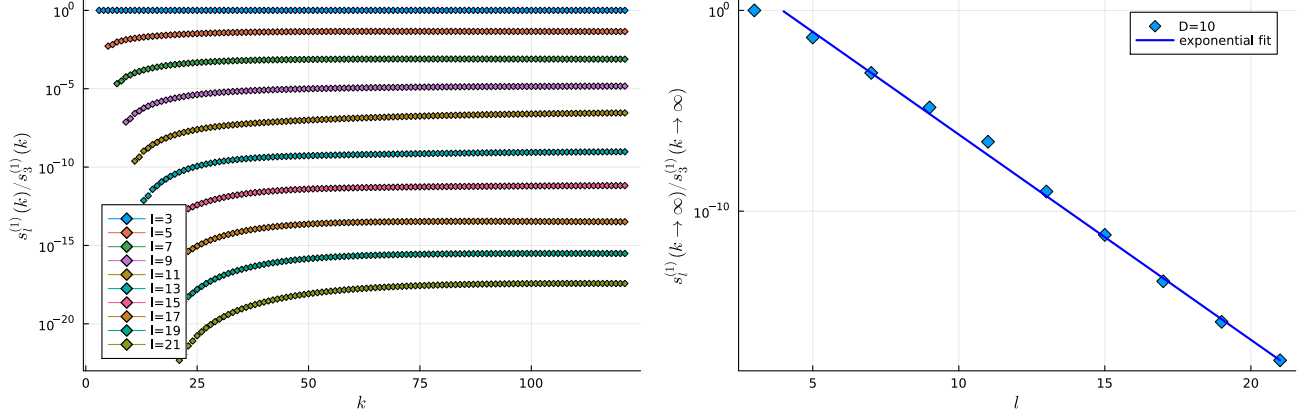


FIG. 7. Anderson model with $D = 10$. Left: Norm ratio $s_l^{(1)}(k)/s_3^{(1)}(k)$ for a fixed l as a function of k . Right: The norm ratio $s_l^{(1)}(k \rightarrow \infty)/s_3^{(1)}(k \rightarrow \infty)$ decays exponentially with the support l . The data are averaged over 100 samples.

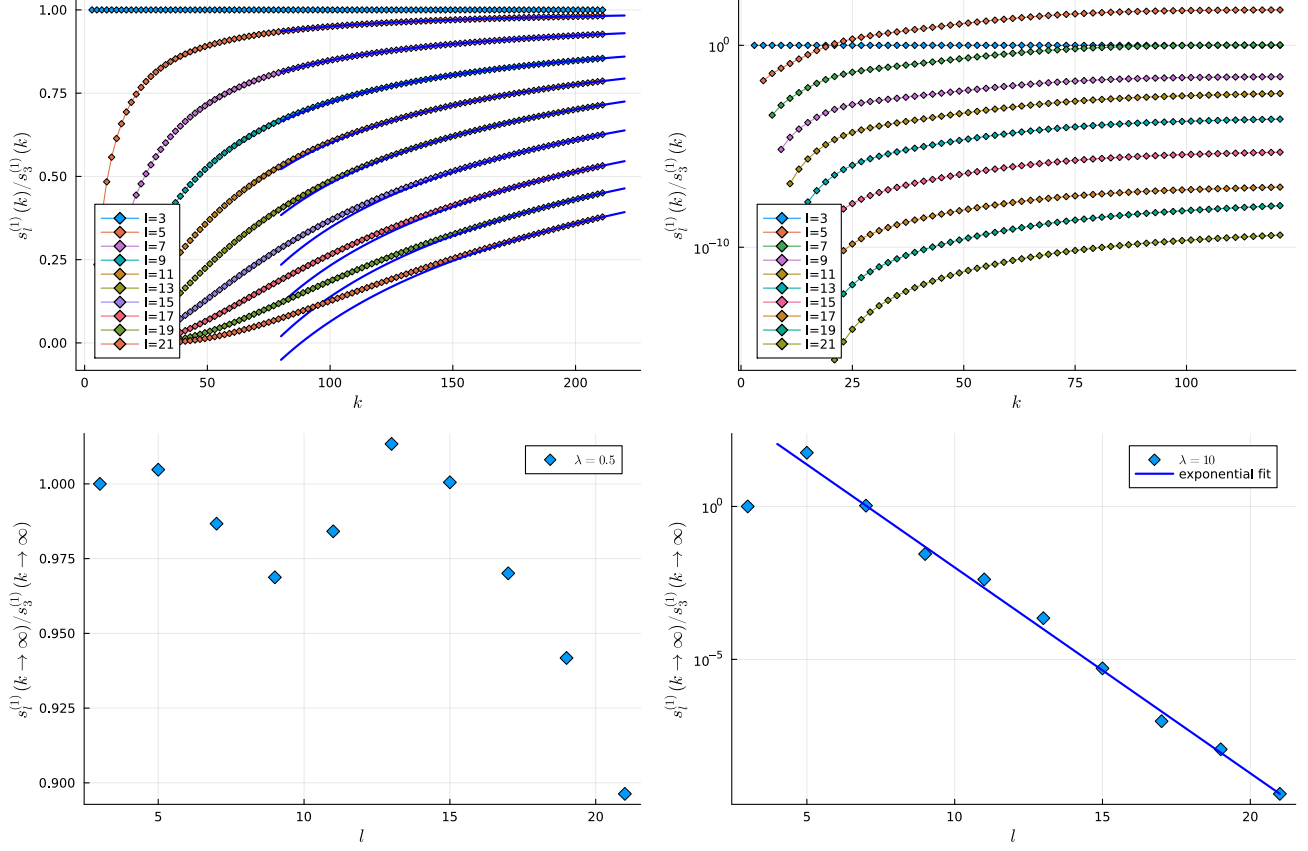


FIG. 8. Aubry-André model for $\beta = (1 + \sqrt{5})/2$, $\phi = 0$ where $\lambda = 0.5$ (left column, linear scale) and $\lambda = 10$ (right column, logarithmic scale). For $\lambda = 0.5$, $s_l^{(1)}(k)$ is extrapolated (blue lines) and the results are consistent with $s_l^{(1)}(k) \sim Ce^k$ with a constant C independent of l . This leads to $s_l^{(1)}(k \rightarrow \infty)/s_3^{(1)}(k \rightarrow \infty) \approx 1$ (bottom left panel) clearly showing that the model is not in the localized phase. In contrast, for $\lambda = 10$ the norm scales as $s_l^{(1)}(k) \sim e^k e^{-l}$, i.e., is exponentially suppressed with increasing l for k fixed, demonstrating that the model is now in the localized phase (bottom right panel).

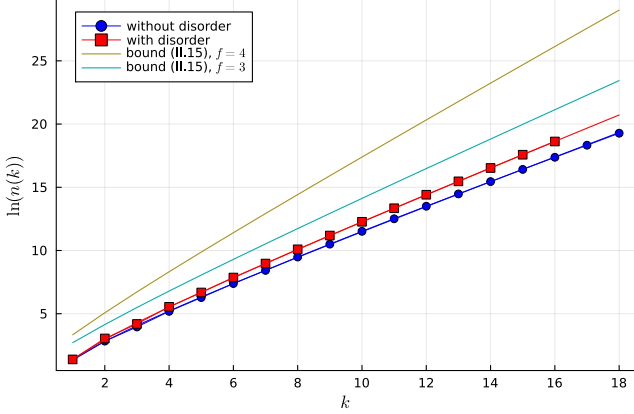


FIG. 9. In the interacting model with $\Delta = 1$, the number of different terms $n(k)$ in the commutator $[H, \sigma_0^z]^{(k)}$ grows exponentially (symbols) and is very well fitted by $n(k) \sim 1.514 k^{0.803} \exp(0.922k)$ in the non-disordered case and $n(k) \sim 1.492 k^{0.815} \exp(0.998k)$ in the case with disorder (solid lines). The general bounds (II.15) with $f = 3$ and $f = 4$ are shown as well.

symmetry is preserved. I.e., we are in any case studying the operator growth of a local operator σ_j^z which belongs to a globally conserved charge. Differences between integrable and non-integrable model are, of course, expected if we study the Euclidean time dynamics of operators of the type $O = \sum_j o_j$ [31]. However, for the Euclidean time dynamics of *local* operators in a generic system, the only thing which matters is whether or not this system has local conserved charges, i.e., whether it is localized or not. We also note that integrability is immediately destroyed if we introduce even an infinitesimal amount of disorder.

We will first briefly consider the case without disorder before turning to the most interesting case, the XXX model with random magnetic fields $h_j \in [-D, D]$ which has been suggested to contain a localized phase for sufficiently strong disorder.

1. No disorder

From the exact solution of the model, we know for sure that the eigenstates of the XXX model are not localized. We can calculate the number of distinct terms $n(k)$ in the commutator $[H, \sigma_0^z]^{(k)}$ at order k by symbolic calculations up to order $k = 18$ exactly. We have not been able to identify the series but asymptotically the number of terms $n(k)$ does grow exponentially with a multiplicative algebraic correction which is consistent with the general bound (II.15) which we derived earlier. The data and a corresponding fit are shown in Fig. 9. The fit works extremely well with a least square deviation of $\chi^2 \sim 10^{-2}$. The local operator basis for the Heisenberg model has dimension $f = 4$ and consists of the operators $1, \sigma^x, \sigma^y, \sigma^z$. We note, however, that only a small subset of terms in

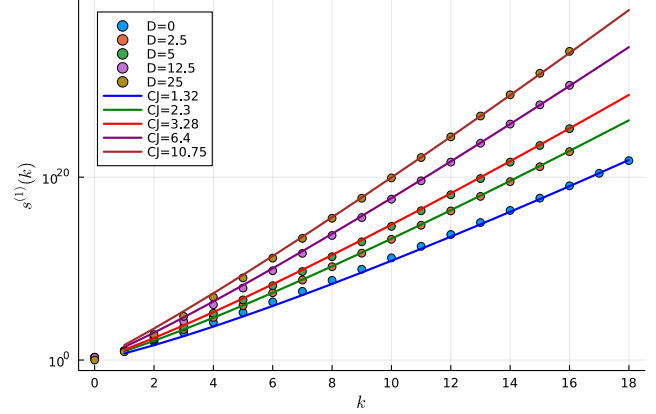


FIG. 10. The 1-norm in the interacting case with $\Delta = 1$ grows faster than exponential for all disorder strengths shown, consistent with the rescaled general bound, Eq. (II.12). The data are averaged over 30 disorder realizations for $D = 2.5$, $D = 5$ and $D = 12.5$ and over 50 realizations for $D = 25$.

$[H, \sigma_0^z]^{(k)}$ contains an identity in between Pauli matrices. Ignoring such terms, we can set $f = 3$ in Eq. (II.15) which gives a much tighter bound, see Fig. 9. The exponential growth of $n(k)$, instead of the quadratic growth in the free-fermion case, indicates that in the corresponding commutator graph the number of nodes per level is no longer constant.

We note that the number of distinct terms is different and always smaller than the number of connected clusters which we have calculated in Eq. (II.11). The reason is that different connected clusters can result in the same term. For the calculation of the norm this does not matter though. We can bound the contribution of each connected cluster as in Eq. (II.12) even if some of the resulting terms are the same. In Fig. 10 we show that this general bound indeed describes the norm growth well if we use the bound on the local Hamiltonian, $\|h_I^a\| \leq J$, as a fitting parameter. In particular, the norm clearly grows faster than exponential for the orders of the commutator which we can handle symbolically. We also note that we obtain qualitatively similar results if we use the 2-norm instead of the 1-norm, see Fig. 11. This difference between the non-interacting and the interacting case becomes even more evident if we consider the norm $s_l^{(1)}(k)$ of terms supported on l sites, see Fig. 12. Whereas in the non-interacting, non-disordered case the norm of the terms supported on l sites grows asymptotically in the same way independent of l if the order of the commutator k is much larger than l , see Eq. (III.12), $s_l^{(1)}(k)/s_1^{(1)}(k)$ has a maximum which shifts to larger and larger l with increasing k in the interacting case. For large k , the total norm is thus completely dominated by terms which have support on a large number of lattice sites. This is to be expected, given that the number of distinct terms in the commutator is increasing exponentially which also leads to a rapidly growing number of possible paths between

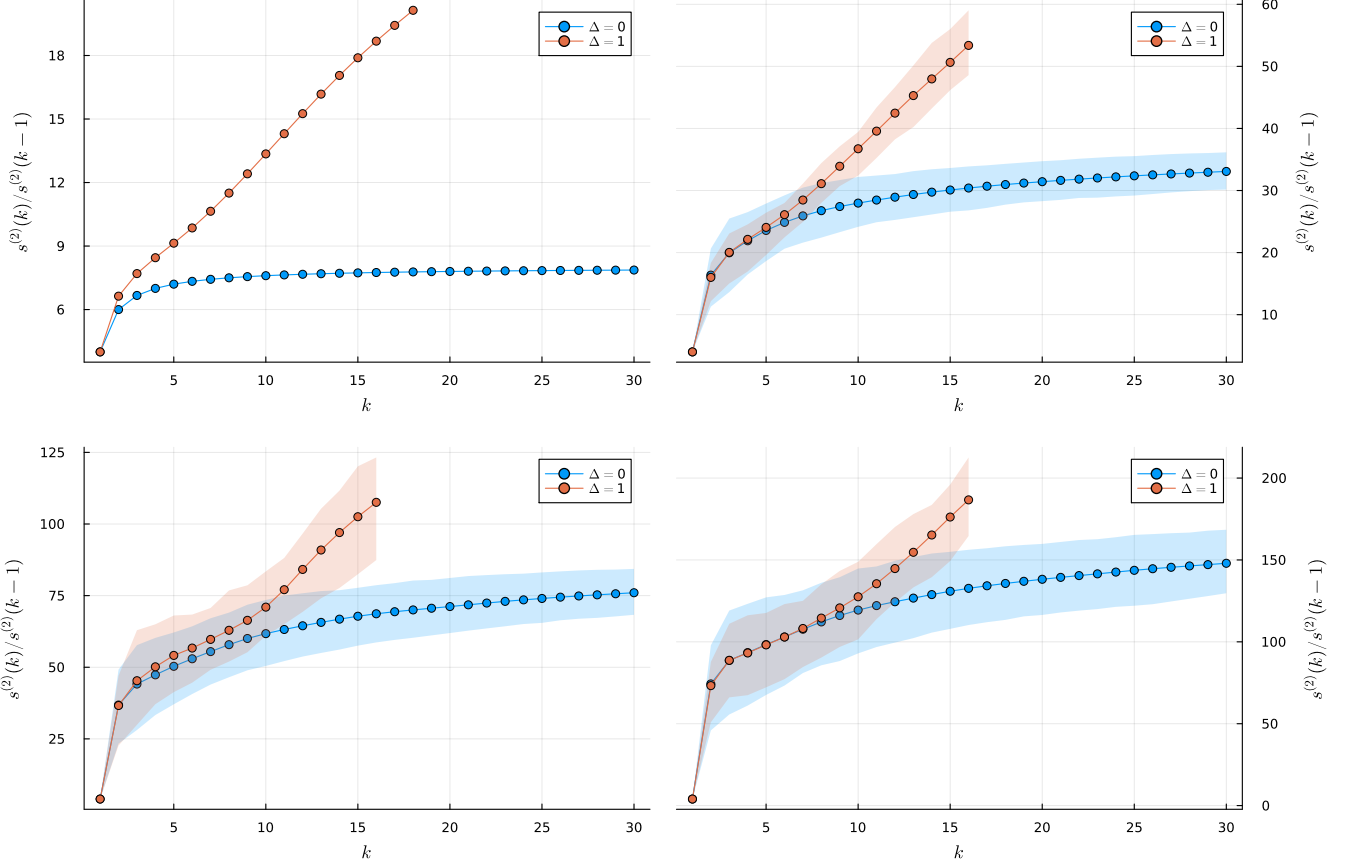


FIG. 11. Average of the 2-norm ratio $s^{(2)}(k)/s^{(2)}(k-1)$ for the XXZ chain with $\Delta = 0$ and $\Delta = 1$ for disorder strengths $D = 0, 5, 12.5, 25$. The data for $D = 5$ and $D = 12.5$ are averaged over 50, and the data for $D = 25$ over 70 realizations. The shaded regions indicate the intervals into which 50% of all realizations fall. The norm ratio has to become a constant for large k if the norm grows exponentially.

those terms, see also the graph in Fig. 13. Note that the graph is no longer regular; the number of edges per node is not constant and is increasing with the level the node is situated on. Note that this increase of the number of edges is a prerequisite for a faster than exponential growth of the norm.

2. Many-body localization

From the perspective of operator spreading, localization in a many-body system is thus an extremely challenging requirement. In a graph with an equal number of edges at each level as realized in a non-interacting model, see Fig. 4, it is easy to see—at least in the limit of large disorder—how the norm of terms with support on only a few sites can dominate the total norm. The exponential growth of edges in the interacting case (see Fig. 13), on the other hand, suggests that the total norm for large k will be entirely dominated by terms with support on many lattice sites. I.e., a local operator is generically expected to delocalize. This aspect also makes it difficult

to see how a perturbative construction of local integrals of motion can be arranged. This is a point which seems to have not been sufficiently appreciated in Refs. [47, 48] where such a construction was suggested. We will get back to this point in Sec. IV. The only way a local operator can avoid to spread through the entire system in the many-body case thus seems to be intricate interference effects between the exponentially many different paths in the graph, Fig. 13. While such fine-tuned destructive interference seems implausible as a generic mechanism for many-body localization we cannot, in general, show that such effects do not exist. We note, however, that for the transverse Ising chain with random fields—the model considered in the proof of MBL in Refs. [47, 48]—a gauge can be defined such that the commutator has a stoquastic-type property [37]. I.e., all terms in the commutator in this gauge have a positive amplitude. For this model, interference effects as a mechanism for localization are thus strictly excluded. For the Heisenberg model considered here, such a gauge does not exist. We will instead consider data from symbolic computations up to order $k = 16$ and show that there is no evidence

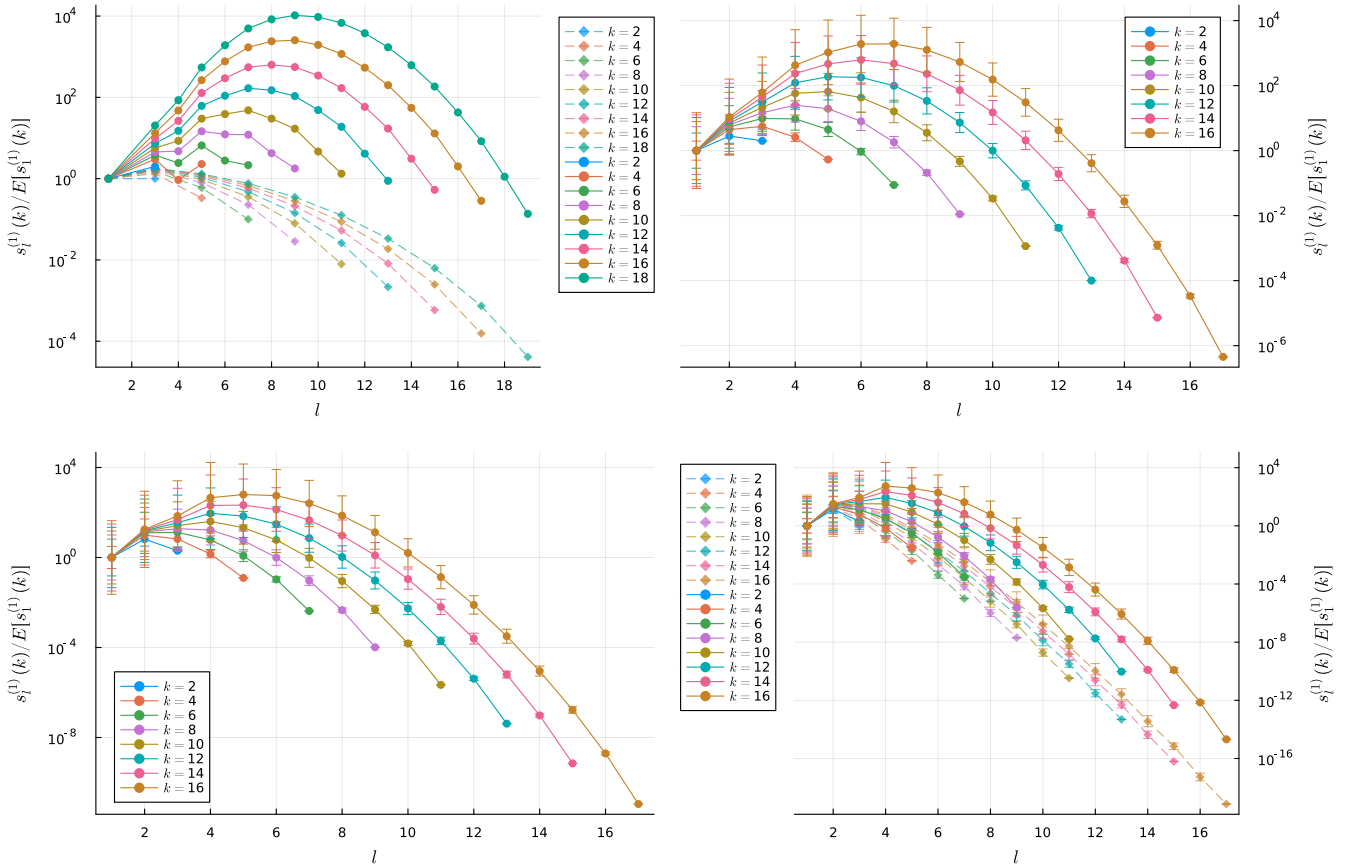


FIG. 12. The norm of operators $s_l^{(1)}(k)/E[s_1^{(1)}(k)]$ with support on l sites for the Heisenberg model with disorder $D = 0, 5, 12.5, 25$. The data for $D = 5$ and $D = 12.5$ are averaged over 50, the data for $D = 25$ over 70 disorder realizations. There is no indication for a convergence with increasing order k to an exponential decay with l even for very strong disorder. For $D = 0$ and $D = 25$ the results for the non-interacting case are shown for comparison (symbols with dotted lines).

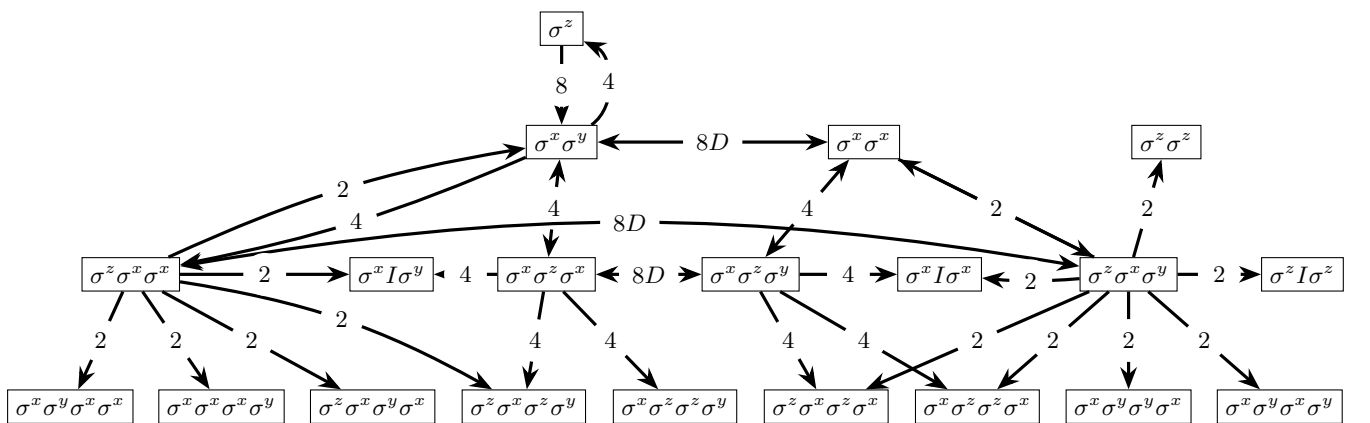


FIG. 13. Graph for the 1-norm $s^{(1)}(k)$ up to order $k = 3$ for the Heisenberg model with random fields $h_j \in [-D, D]$. The number of nodes grows exponentially with the length of the support.

for destructive interference effects and a corresponding localization. We note that at order k , we are considering operators which are spread over $2k + 1$ sites in the lattice. I.e., at order $k = 16$ we are dealing effectively with a chain of 33 lattice sites which is well beyond what is

possible in exact diagonalizations. We will also consider disorder strengths up to $D = 25$ which is much larger than the critical values which have been suggested in the past [8, 10, 11, 49].

Let us start by considering the number of distinct

terms in the commutator at order k which is shown in Fig. 9. We find that the number of terms grows faster in the disordered than in the case without disorder. This is easy to understand: additional terms appear in the commutator due to the random magnetic field terms while all the terms present before remain. The different classes of terms which appear up to order $k = 3$ are shown in the graph in Fig. 13. Next, we consider the growth of the total norm which should be at most exponential in a localized phase as we have proven in Eq. (II.21), see also App. A. The data, however, are overall much better described by the general bound (II.12) than by an exponential, with the norm bound of the local Hamiltonian, $\|h_I^a\| \leq J$, used as a fitting parameter. While this does not exclude the possibility that for larger k the scaling eventually does become exponential, we can say with confidence that no indications for localization are observed in spin chains up to 33 sites. These system sizes are much larger than those used in exact diagonalizations, the method which claims of a many-body localized phase have been mostly based on [8, 10, 11, 19]. The stronger than exponential growth of the norm is further supported by considering the ratio of norms $s_l^{(2)}(k)/s_3^{(2)}(k-1)$ which is shown in Fig. 11. For the orders of the commutator which we can handle symbolically, there is no indication that this norm ratio saturates, even for extremely strong disorder, as it has to in a localized case where $s(k) \sim \exp(k)$. As the figure shows, the behavior in the interacting case is in stark contrast to the localized non-interacting case.

Finally, let us also consider the norm ratio $s_l^{(1)}(k)/E[s_1^{(1)}(k)]$ of terms with support on l sites which is shown in Fig. 12 for various disorder strengths. Here $E[s_1^{(1)}(k)]$ denotes the mean of terms with support on one site. Even for very strong disorder $D = 25$ there is no indication of a convergence to an exponential decay with l . To the contrary, there is always a maximum which shifts to larger l with increasing order k just as in the case without disorder. To further highlight this point, we show in Fig. 14 the norm ratio $s_l^{(1)}(k)/s_3^{(1)}(k)$ as a function of the order k for various fixed l . In contrast to the non-interacting case shown in Fig. 7, the curves do not saturate for large k but rather are consistent with the weight in the total norm shifting to larger and larger l with increasing k . While we cannot exclude that this trend changes for even larger k than the ones we can handle in symbolic calculations, we want to stress once more that the terms in the commutator are spread over 33 sites for $k = 16$. This is already much larger than the system sizes typically considered in exact diagonalizations. At the very least, we can say that for chains of lengths up to 33 sites, there is no indication that a many-body localized phase will be realized even at disorder strengths up to $D = 25$.

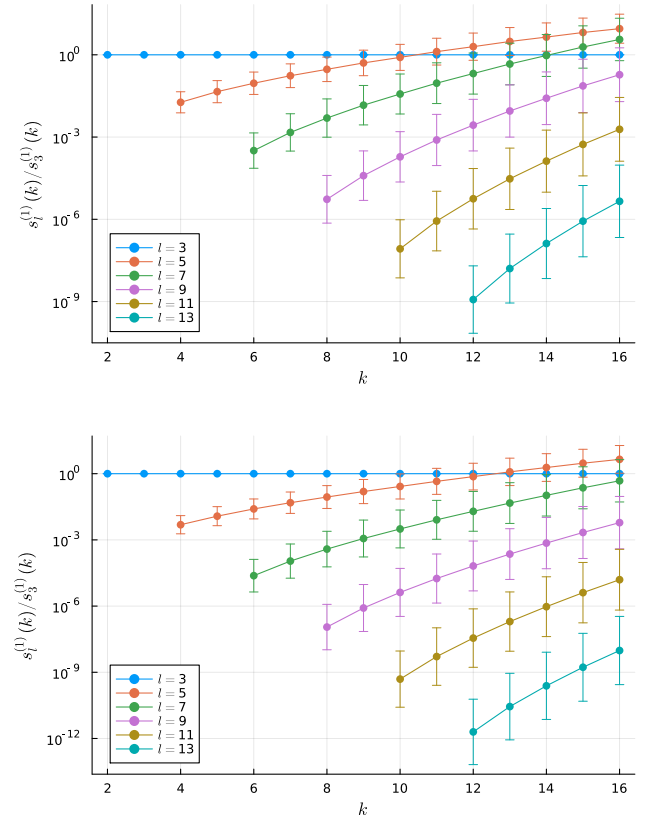


FIG. 14. Norm ratio $s_l^{(1)}(k)/s_3^{(1)}(k)$ for a fixed l as a function of k for the Heisenberg model with $D = 12.5$ (top) and $D = 25$ (bottom). These results are to be compared with the non-interacting case shown in Fig. 7.

IV. SCHRIEFFER-WOLFF TRANSFORMATIONS

We have so far considered the commutator of a microscopic lattice Hamiltonian H with a local operator σ_i^z . If this Hamiltonian is in a localized phase, then it is unitarily equivalent to a Hamiltonian of (interacting) conserved charges τ_j^z which are localized around lattice site j , see Eq. (I.2). Our argument has been that the local operator σ_i^z then only has significant overlap with conserved charges τ_j^z which are localized near site i . Thus, the operator σ_i^z will remain localized—up to exponential tails—under Euclidean time evolution.

An alternative but related approach is to try to explicitly construct the unitarily equivalent Hamiltonian written in terms of local conserved charges τ_j^z [29, 47, 48, 50–52]. It is important to note that these charges are not uniquely defined: if, for example, τ_j^z and τ_{j+1}^z are conserved charges localized near lattice site j with $[H, \tau_j^z] = [H, \tau_{j+1}^z] = 0$ then $\tau_j^z \tau_{j+1}^z$ is also local and conserved, $[H, \tau_j^z \tau_{j+1}^z] = 0$.

One way to obtain these charges is to try to perturbatively construct them in the limit of strong disorder

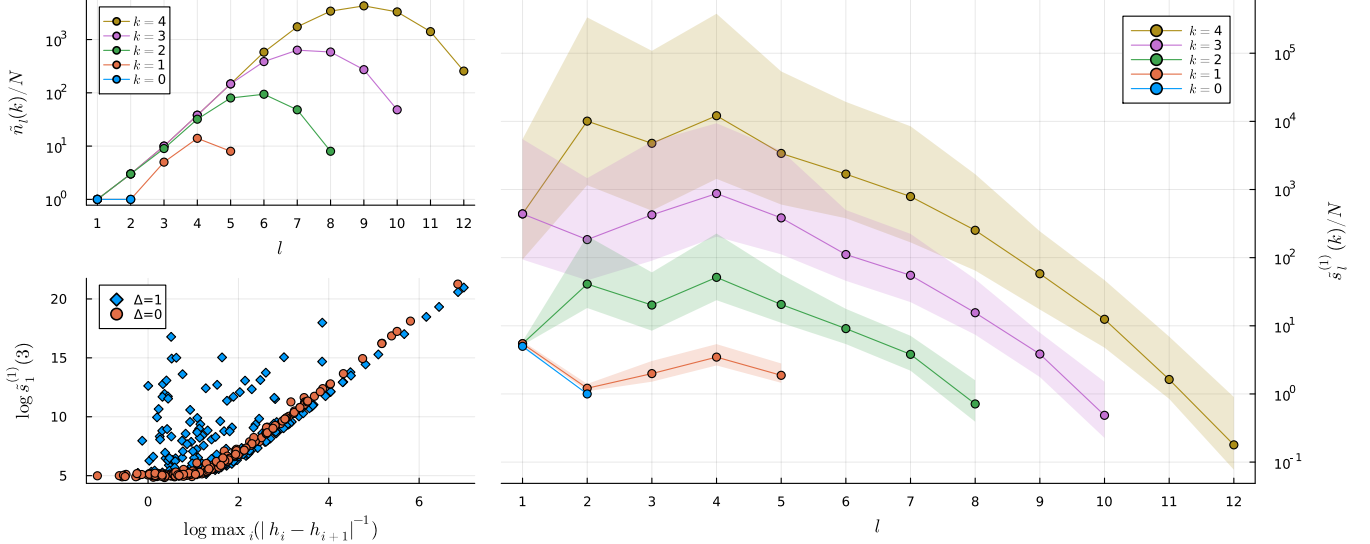


FIG. 15. Top left: Number of terms in the Hamiltonian with support on l sites after performing the Schrieffer-Wolff transformation (IV.9) up to order k for the XXX chain with disorder and $N = 100$ lattice sites. For large k , this number increases approximately exponentially with l . Note that $\tilde{n}_l(k)$ does not depend on the disorder realization; the results are exact. Bottom left: Total norm of terms with support on one site after $k = 3$ transformations for 200 samples versus $\max_i |h_i - h_{i+1}|^{-1}$. Right: Total norm of terms with support on l sites after k transformations averaged over 200 realizations for $N = 100$ and $D = 5$. While each term is expected to have an amplitude $\sim D^{-2l}$ if there are no resonances, the exponentially increasing number of terms means that the total coupling of distant sites is no longer controlled by a small parameter. For example, we have $\tilde{s}_1^{(1)}(k) \approx \tilde{s}_8^{(1)}(k)$ for $k = 4$.

[47, 48, 50]. In this limit, one can think of these charges as the local operators σ_i^z smeared out by the hopping and dressed by the interactions. As in our previous considerations, there is then again an important difference between the non-interacting and the interacting case: While in the former the one-particle operators $\sigma_i^z = c_i^\dagger c_i - 1$ remain one-particle operators, they become many-particle operators in the latter case. As we will see, the perturbative transformation of the Hamiltonian will lead us again to multiple commutators which are closely related to the ones studied in the previous sections.

The Hamiltonian of a quantum system can be diagonalized by a unitary transformation

$$H \rightarrow \exp(T)H\exp(-T) = \sum_{k=0}^{\infty} \frac{[T, H]^{(k)}}{k!} \quad (\text{IV.1})$$

with $T^\dagger = -T$ being an anti-unitary operator. For a Hamiltonian $H = H_0 + V$ where H_0 is diagonal in the operator basis chosen, we can instead of a full diagonalization demand that the new Hamiltonian $H^{(1)}$ is diagonal only to first order in the perturbation V . This is the Schrieffer-Wolff transformation [53, 54]. Going one step further, we can consider successive Schrieffer-Wolff transformations where in each step the perturbation is eliminated to leading order. This is closely related to the approach in Ref. [47, 48] which tries to generalize a proof of Anderson localization to the many-body case. In these works, the author is mostly concerned with the impact of resonances and splits the off-diagonal part of

the Hamiltonian into a resonant and a non-resonant part. We will discuss the impact of resonances as well but will point out an even more fundamental issue which calls into question the entire perturbative construction of local conserved charges in the interacting case even for disorder configurations where no resonances are present.

To be specific, we consider again the XXZ Hamiltonian (III.1). We note that in Refs. [47, 48] the transverse field Ising model with random couplings and random fields was considered instead. However, the arguments made in the following are quite general and will apply to the latter model as well [37]. We want to investigate the case of large disorder where the magnetic field and the interaction terms constitute H_0 with $[H_0, \sigma_i^z] = 0$ and the hopping terms are the perturbation. The condition the operator T has to fulfill to lowest order is then given by

$$V + [T, H_0] = 0 \quad (\text{IV.2})$$

and the new, transformed Hamiltonian is obtained as

$$H^{(1)} = H_0 + \frac{1}{2}[T, V] + \frac{1}{3}[T, [T, V]] + \dots \quad (\text{IV.3})$$

In the Schrieffer-Wolff transformation, one typically stops at the first order correction to H_0 . To justify this perturbative approach, we can rescale the Hamiltonian (III.1) by $1/D$ which changes the energy scales but leaves the physical properties unchanged. Then, the hopping terms have an amplitude $J_{j,j+1}^{(0)} = 1/D$ and the interaction

terms an amplitude $\bar{\Delta} = \Delta/D$ which are both small parameters for large D . After this rescaling, the random magnetic fields are always given by $h_j \in [-1, 1]$.

A. Non-interacting case

First, we consider again the non-interacting case. An ansatz for the operator T can be obtained by commuting H_0 and V . This leads to $T = \sum_j A_j (\sigma_j^+ \sigma_{j+1}^- - \sigma_{j+1}^+ \sigma_j^-)$. The amplitudes A_j can then be determined from Eq. (IV.2) leading to

$$T = \frac{1}{2} \sum_j \frac{\bar{J}_{j,j+1}^{(0)}}{h_j - h_{j+1}} (\sigma_j^+ \sigma_{j+1}^- - \sigma_{j+1}^+ \sigma_j^-). \quad (\text{IV.4})$$

We note that the Schrieffer-Wolff operator T is thus proportional to the spin current operator $\mathcal{J} = \sum_i j_i$ which can be obtained from the lattice continuity equation [55]

$$\partial_t \sigma_i^z = -i[\sigma_i^z, H] = -(j_i - j_{i-1}). \quad (\text{IV.5})$$

We note, furthermore, that $|\overline{h_{j+1} - h_j}| = 2/3$, i.e., the factor $\bar{J}_{j,j+1}^{(0)} / |h_j - h_{j+1}|$ is small on average if the disorder strength D is large. However, if two neighboring sites have roughly the same potential, then this factor can become large or might even diverge. Rare resonances thus might destroy the perturbative construction if they proliferate. An example how such resonances can affect the transformed Hamiltonian is shown in Fig. 15, bottom left panel. We will come back to this point below.

After the Schrieffer-Wolff transformation, the new Hamiltonian is given by

$$\begin{aligned} H^{(1)} &= H_0^{(0)} + \frac{1}{2} [T^{(0)}, V^{(0)}] + \frac{1}{3} [T^{(0)}, [T^{(0)}, V^{(0)}]] \\ &= \sum_j \left\{ \bar{J}_{j,j+2}^{(1)} (\sigma_j^+ \sigma_{j+1}^z \sigma_{j+2}^- + \text{h.c.}) + 2h_j^{(1)} \sigma_j^z \right\} \\ &\quad + \sum_j \bar{J}_{j,j+1}^{(1)} (\sigma_j^+ \sigma_{j+1}^- + \text{h.c.}) \end{aligned} \quad (\text{IV.6})$$

with $H_0^{(0)} = H_0$, $V^{(0)} = V$, and $T^{(0)} = T$. The coupling constants and renormalized fields are given by

$$\begin{aligned} \bar{J}_{j,j+2}^{(1)} &= \frac{(\bar{J}_{j,j+1}^{(0)})^2}{2(h_{j+1} - h_j)} + \frac{(\bar{J}_{j,j+1}^{(0)})^2}{2(h_{j+1} - h_{j+2})} \quad (\text{IV.7}) \\ h_j^{(1)} &= h_j^{(0)} + \frac{(\bar{J}_{j,j+1}^{(0)})^2}{4(h_j - h_{j-k})} + \frac{(\bar{J}_{j,j+1}^{(0)})^2}{4(h_j - h_{j+1})} \end{aligned}$$

and $\bar{J}_{j,j+1}^{(1)} \sim 1/D^3$ (the exact expression is lengthy and not needed in the following). The first two terms correspond to those generated by $[T^{(0)}, V^{(0)}]$ while the renormalized nearest-neighbor hopping $\bar{J}_{j,j+1}^{(1)}$ stems from the next higher commutator $[T^{(0)}, [T^{(0)}, V^{(0)}]]$. I.e., the transformation to lowest order eliminates the

nearest-neighbor hopping processes but generates a next-nearest neighbor hopping $\bar{J}_{j,j+2}^{(1)} \sim 1/D^2$ (note that $\sigma_j^+ \sigma_{j+1}^z \sigma_{j+2}^- + \text{h.c.} = c_j^\dagger c_{j+2} + \text{h.c.}$ in the fermionic language) and renormalizes the local fields $h_j^{(0)} \rightarrow h_j^{(1)}$.

If we stop at the leading order of the transformation, then we obtain a Hamiltonian $H^{(1)}$ which looks like the original Hamiltonian $H^{(0)}$ but with the nearest-neighbor hopping replaced by a weaker next-nearest neighbor hopping. We can then again define a Schrieffer-Wolff transformation to eliminate these next-nearest hopping terms which has the form

$$T^{(k)} = \frac{1}{2} \sum_j \frac{\bar{J}_{j,j+k+1}^{(k)}}{h_{j+k+1}^{(k)} - h_j^{(k)}} (\sigma_j^+ \sigma_{j+1}^z \dots \sigma_{j+k}^z \sigma_{j+k+1}^- - \text{h.c.}) \quad (\text{IV.8})$$

with $k = 1$. This will again, to leading order, renormalize the local fields and generate a third-nearest neighbor hopping which again can be eliminated to leading order by a the Schrieffer-Wolff transformation (IV.8) with $k = 2$. I.e., we can define a series of successive Schrieffer-Wolff transformations which lead to longer and longer range interactions which are, however, suppressed as D^{-2k} . At the same time, they define an exponentially converging series for the renormalized random fields $h_j^{(k)}$. If there are no resonances, then we can drop the hopping term when all the amplitudes $J^{(k)}$ have fallen below some threshold, giving us an effective Hamiltonian with renormalized magnetic fields. In this approximation, which can be justified at very strong disorder and which corresponds to summing up exactly certain classes of diagrams, the conserved local charges are just the σ_j^z themselves but with renormalized amplitudes. This can be seen as a consistency check that at very large disorder such an effective description exists because the hopping is an irrelevant perturbation.

In the non-interacting case, it is also well understood that distance resonances have a vanishingly small probability to proliferate [1, 3, 4]. In our construction, this scaling argument arises as follows: Two lattice sites j and $j+\ell$ a distance ℓ apart are coupled by an effective long-range hopping $\bar{J}_{j,j+\ell}^{(\ell-1)} (c_j^\dagger c_{j+\ell} + \text{h.c.})$ with an effective amplitude obtained by $\ell-1$ successive Schrieffer-Wolff transformations. The amplitude of this long-range effective hopping term is given by $\bar{J}^{(\ell-1)} \sim D^{-2\ell+2} \times f[\{(h_j^{\ell-1} - h_k^{\ell-1})^{-1}\}]$ where f is some function of the inverse differences of the random fields within the cluster of ℓ sites. Now the smallest pairwise difference on this cluster on average scales as ℓ^{-2} . Thus the effective long-range hopping amplitude scales as $\bar{J}_{j,j+\ell}^{(\ell-1)} \sim D^{-2\ell} \ell^2$ and is thus typically exponentially suppressed. Therefore resonances have a vanishingly small probability to proliferate and to destroy the perturbative construction above. This is also supported by our symbolic calculations on finite chains of length N . First, we note that the size of the norm of terms with support on one site is entirely determined by how close to a nearest-neighbor resonance a given sample is. Distant resonances play no role; all the data fall onto a 'hockey

stick' curve, see Fig. 15, bottom left panel. Second, we consider successive lowest order Schrieffer-Wolff transformations and stop the transformations if the total 1-norm of the off-diagonal part is below some threshold value ε . We have $\sim N$ possible off-diagonal terms of a given range and if the amplitudes of all those terms, on average, are suppressed as D^{-2k} at order k of the transformation then our condition to stop is $ND^{-2k} < \varepsilon$. We thus expect that we need $k \sim \ln(N/\varepsilon)$ many transformation steps. This is consistent with our observations.

Quite generally we may ask why we expect a perturbative construction of the local conserved charges to work in the non-interacting case? In the lowest-order construction discussed above, the Hamiltonian $H^{(k)}$ always has $3N$ terms for a chain of length N for every k . I.e., the number of terms does not increase during successive Schrieffer-Wolff transformations. If we take higher order commutators in the transformation into account, then the number of terms will increase, however, the Hamiltonian $H^{(k)}$ and the transformation $T^{(k)}$ will always consist of a sum of one-body operators and, for a chain of length N , there are only N^2 distinct one-body operators. Therefore the problem of finding local conserved charges is at most quadratic, and, in any finite order approximation, one in fact always deals with a constant, non-increasing number of terms in the transformed Hamiltonians.

B. Interacting case

The interacting case, on the other hand, is completely different and none of the above arguments hold. We are, however, able to generalize Eq. (IV.4) and to obtain the exact Schrieffer-Wolff transformation for the XXZ chain and arbitrary interaction strength Δ . We find

$$\begin{aligned} T = & \sum_j \frac{\bar{J}_{j,j+1}^{(0)}(\sigma_j^+ \sigma_{j+1}^- - h.c.)}{2(h_j - h_{j+1})(2\bar{\Delta}^2 - 2(h_j - h_{j+1})^2)} \\ & \times [\bar{\Delta}^2 - 2(h_j - h_{j+1})^2 + \bar{\Delta}^2 \sigma_{j-1}^z \sigma_{j+2}^z + \bar{\Delta}(h_j - h_{j+1})(\sigma_{j-1}^z - \sigma_{j+2}^z)] \end{aligned} \quad (\text{IV.9})$$

with $\bar{J}_{j,j+1}^{(0)} = 1/D$ and $\bar{\Delta} = \Delta/D$. We note that for $\Delta \neq 0$, the transformation T consists of $8N$ distinct operators for a chain of length N , including operators acting on 2, 3 and 4 neighboring sites.

If we stop the transformation (IV.3) at first order, the transformed Hamiltonian $H^{(1)}$ already has $29N$ distinct operators if the chain length N is sufficiently large. This includes terms acting on 5 neighboring sites but also terms such as $\sigma_j^z \sigma_{j+1}^z$ and $\sigma_j^z \sigma_{j+2}^z \sigma_{j+3}^z$. Even for very strong disorder, the transformation thus does not just lead to a renormalization of the random fields but necessarily leads to a broadening of the diagonal basis. Symbolically, we can also construct $T^{(1)}$ to eliminate the off-diagonal terms in $H^{(1)}$. We find that $T^{(1)}$ already consists of $786N$ distinct operators. The transformed Hamiltonian $H^{(2)}$ then has $30618N$ many terms. I.e., even if we

stop the Schrieffer-Wolff transformation at lowest order, the number of terms in $T^{(k)}$ and $H^{(k)}$ is growing exponentially. Furthermore, there is no distinct set of diagrams which we can simply sum up to all orders. Exponentially many new diagrams are created at each order.

The related and most fundamental problem, however, is that lattice sites j and $j + \ell$ a distance ℓ apart will be coupled by $\sim 3^2 4^{\ell-1}$ distinct operators because on each site we can put in principle one of the operators $\{\sigma^x, \sigma^y, \sigma^z, \mathbb{I}\}$ but the string of operators of length $\ell + 1$ has to start and end with one of the three Pauli matrices. While not all of these combinations of operators will be realized in a microscopic model such as the XXX chain, there will be exponentially many distinct operators which couple these two sites, see Fig. 15. Thus there is, in general, no reason to expect this perturbative construction to work because the overall effective amplitude of terms coupling these two sites will be $\bar{J}_{j,j+\ell} \sim D^{-\ell} 4^\ell \sim \mathcal{O}(1)$. I.e., there is no small parameter anymore. This reasoning is supported by the results of symbolic calculations shown in Fig. 15. Here we have calculated the sum $\tilde{s}_\ell^{(1)}(k)$ of the amplitudes of all terms obtained in the Schrieffer-Wolff transformation (IV.9) to order k which have support on ℓ sites, i.e., which connect sites a distance $\ell - 1$ apart. For a periodic chain with even length N , there are $\sim N$ distinct pairs of sites which are a distance $1, \dots, N/2$ apart. I.e., for a specific pair the overall coupling is on average $\sim \tilde{s}_\ell^{(1)}(k)/N$ and, as can be seen in Fig. 15, is in general not exponentially decreasing with ℓ . That the number of terms generated in such a transformation with support on ℓ sites is exponentially increasing with ℓ makes it very questionable that a construction of local conserved charges in this perturbative manner is a controlled approximation. This is a major issue even before thinking about the problem of resonances and thermal inclusions (regions for a given disorder configuration which, by chance, are only weakly disordered). It seems to us that the exponential increase of the number of terms in such transformations is a point which has not been properly addressed in the proof of MBL in Refs. [47, 48] where the author seems to be only concerned about the effect of resonances. While it is not impossible that for disorder configurations without resonances and thermal inclusions the perturbative construction of local charges is working in the thermodynamic limit—for example, because of interference effects between different terms coupling the same sites—any proof needs to provide rigorous arguments that the exponentially many terms do not overwhelm the exponential small parameter in the expansion. Such arguments seem to be missing so far. We note that for a finite system the construction will always eventually converge because the finite length provides a cutoff and $\tilde{s}_\ell^{(1)}(k)$ will eventually drop off exponentially with ℓ .

The destabilizing effects of resonances and thermal inclusions have received considerable attention in the literature already [42, 56, 57]. From the perspective of perturbative Schrieffer-Wolff transformations, they lead to the following additional problems: The renormalized

couplings for an operator acting on ℓ lattice sites will in its denominator typically contain a linear combination of *all* the random fields on these ℓ sites. Given that there are exponentially many such operators, the simple scaling argument for the non-proliferation of resonances in the Anderson case is clearly no longer applicable in the interacting case. This can be seen in Fig. 15, bottom left panel, where the sum of the amplitudes of terms in the Hamiltonian with support on one site, $\tilde{s}_1(k)$, in the interacting case is large even for samples which do not have nearest-neighbor resonances. Thermal inclusions—regions of the lattice which have similar potentials—lead, furthermore to an additional destabilization of the perturbative transformation. This can be seen, for example, in symbolic calculations of the unitary transformation (IV.1) with the operator (IV.9) to higher orders. In configurations where such regions exist, the transformation generates long-range terms with large amplitudes even if the disorder D is extremely strong. If, on the other hand, we exclude configurations with such regions and with any pairwise resonances by hand, then the amplitudes of any individual operator typically decay with the length of its support. Another manifestation of this issue can be seen when performing k successive lowest order Schrieffer-Wolff transformations for a finite chain of length N . We want to stop the transformations again once the 1-norm of the off-diagonal part is below some threshold ε . In contrast to the non-interacting case, we now have exponentially many terms connecting sites a given distance apart. If we assume that individual amplitudes in the off-diagonal part are suppressed as D^{-2k} , then the condition for stopping the transformations becomes $e^N D^{-2k} < \varepsilon$ and we would thus expect that we need $k \sim N$ steps for N sufficiently large. This is, however, not what we observe for typical disorder configurations. The results of our symbolic calculations point instead to an increase of the number of transformations $k \sim e^N$. This implies that some amplitudes in the off-diagonal part are $\sim \mathcal{O}(1)$ and that we have to eliminate almost all of the off-diagonal terms to achieve convergence.

In summary, the iterative transformation of the Hamiltonian cannot simply be transferred from the non-interacting to the interacting case. There are two main issues: Even if one considers only a lowest order transformation, one is not dealing with a constant number of operators but rather with an exponentially increasing number of operators, both in the Schrieffer-Wolff transformation $T^{(k)}$ as well as in the transformed Hamiltonian $H^{(k)}$. Even if one tries to only perform a single unitary transformation (IV.1) with the operator T , the number of distinct operators in the transformed Hamiltonian is increasing exponentially with the support of the operator which thus can overwhelm the exponential decay of the amplitude of individual operators with the length of their support. We note that different but related arguments for the failure of a perturbative construction of conserved charges in the interacting case have recently been made

in Ref. [58]. Furthermore, regions with similar lattice potentials result in individual operators with large support which, nevertheless, have large amplitudes even for very strong disorder. The latter issue is related to the well-known avalanche instability [42, 56, 57, 59].

V. CONCLUSIONS

We have considered operator growth in one-dimensional lattice models and its connection to localization from two different perspectives. First, we studied the multiple commutator $[H, A]^{(k)}$, which appears in the Euclidean time evolution, for a local operator A and a Hamiltonian H which is a sum of nearest-neighbor terms. For a generic, ergodic system, we have shown that the number of distinct terms generated is exponentially increasing with the order k of the commutator. This leads to a strict bound for the commutator norm $s(k)$ which grows faster than exponential with k , a result which was first demonstrated in Ref. [30]. Since this result is based on a simple counting of connected clusters generated by the commutator, it is expected that this bound is asymptotically tight for an ergodic system. This *operator growth hypothesis* is challenged by results for systems such as the random transverse Ising chain which are supposed to have a localized phase but, nevertheless, always show almost factorial operator growth. Here we systematically addressed this issue. We started by providing strict bounds for two special cases. First, we considered the Hamiltonian H of a free-fermion system. In this case, all the terms generated by the commutator of the Hamiltonian with a one-body operator A will also always be one-body operators. For a short-range Hamiltonian, the spatial range of operators generated at order k will be proportional to k . The number of distinct terms in the commutator can therefore only grow $\sim k^2$ as compared to the exponential growth in the general, interacting case. We also proved an exponential bound for the commutator norm in this case. Second, we considered a localized system, either interacting or non-interacting, and showed that an exponential bound for $s(k)$ exists in this case as well. Physically, this can be understood as follows: a localized system has a set of local conserved charges and the Hamiltonian can be written in terms of these charges. Commuting the Hamiltonian with a local operator A then only involves those charges localized near the site the operator A is acting on. Thus, up to exponential tails, only operators with support on a number of sites which is less than the localization length will significantly contribute to the norm. We note that an almost factorial versus an exponential growth of the commutator norm also leads to distinctly different Lieb-Robinson bounds and asymptotic behavior of matrix elements in the energy eigenbasis. This is further discussed in App. B and App. C.

To distinguish a localized interacting or non-interacting system from a non-localized free fermion sys-

tem, it is important to look beyond the overall norm which has an exponential bound in both cases. Here we have shown that for a non-localized free-fermion system at large commutator order k , the norm $s_l(k)$ of terms which have support on l sites will grow exponentially with k and is *independent* of the length of the support l . In contrast, the norm scales as $s_l(k) \sim \exp(k) \exp(-l)$ for a localized system. I.e., at a fixed order k , the contribution of terms in the commutator is exponentially suppressed with the length of their support l .

We thus have proven sharp criteria to distinguish between free-fermionic localized and non-localized and interacting localized and non-localized systems based on the growth of the total commutator norm $s(k)$ and the contributions $s_l(k)$ to this norm by operators with support on l sites. To illustrate our results, we then considered specific microscopic examples, namely the XX chain (nearest-neighbor free-fermion model), the Anderson model, the Aubry-André model, and the XXX (Heisenberg) chain with and without quenched disorder. For the XX case we have demonstrated that a complete, exact result for the commutator $[H, \sigma_0^z]^{(k)}$ to all orders k can be derived. These exact results confirmed and illustrated our general results derived earlier. For the Anderson model, we derived an exponential bound for the total norm which does depend on the disorder strength D . Based on a graph theoretical approach, we also showed that $s_l(k) \sim \exp(-l)$ for fixed k . I.e., the contribution of terms in the commutator to the total norm is indeed exponentially suppressed with the length l of their support. As another example, we considered the Aubry-André model which has a transition from a non-localized to a localized phase at some finite strength of the applied incommensurate lattice potential. Importantly, we could demonstrate that the non-localized and localized phases of the model can clearly be distinguished by considering the norm $s_l(k)$.

Having checked our results for non-interacting cases, we then turned to the Heisenberg (XXX) chain with quenched disorder. This model has been suggested to have a transition from an ergodic to a many-body localized phase at some finite disorder strength D . In particular, for the MBL phase an effective Hamiltonian written in terms of localized conserved charges is supposed to exist as in the Anderson case but with couplings between these charges which are exponentially decaying with distance. If true, then our proof for localized phases applies. Thus $s(k)$ can grow at most exponentially in such a phase and $s_l(k) \sim \exp(-l)$ at fixed k . We used symbolic calculations of the commutator and were able to reach order $k = 16$ at which point we are considering terms located on a lattice of $2k + 1 = 33$ sites. This is substantially larger than what can be done using exact diagonalizations. We found that the growth of the norm of the commutator $s(k)$ appears to be faster than exponential and consistent with the generic, ergodic bound for non-localized systems for all considered disorder strengths up to $D = 25$. Similarly, we find no indication that $s_l(k) \sim \exp(-l)$. To the

contrary, we find that $s_l(k)/s_1(k)$ has a maximum which appears to shift to larger and larger l with increasing k . At the very least, we claim that our results clearly demonstrate that there is no convincing case for an MBL phase for system sizes up to 33 sites and disorder strengths up to $D = 25$.

As a second approach, we considered unitary Schrieffer-Wolff transformations of the entire Hamiltonian to perturbatively eliminate the hopping terms and construct local conserved charges. We showed that such an approach will succeed in the Anderson case because the Hamiltonian in this case consists of one-body operators and this property is not changed by unitary transformations. Consequently, there are only two terms possible in the effective Hamiltonian which can couple two sites j and k : $c_j^\dagger c_k$ and $c_j c_k^\dagger$. This allows to define consecutive lowest order Schrieffer-Wolff transformations and to sum up the entire series. In this approximation, valid at very strong disorder, the local conserved charges are simply the σ_j^z operators with renormalized fields. The longer-range hoppings generated by the transformations have amplitudes which decay exponentially with the range of the hopping process. The minimum gap between random fields on a cluster of length ℓ on the other hand—which enters the effective hopping in the denominator—scales as ℓ^{-2} and thus cannot overcome the general suppression of the hopping process which scales as $D^{-2\ell}$. This means, in particular, that resonances cannot proliferate.

All of this changes drastically once interactions are included. In particular, there are then $\sim 4^\ell$ different terms which can connect sites a distance ℓ apart. We confirm this exponential growth with the length of the support by symbolic calculations. A priori, there is thus no reason to believe that a perturbative construction of the local conserved charges by unitary transformations is still possible in the interacting case. Even if we assume that there are no resonances or thermal inclusions (regions with random fields of similar strengths), there is a fundamental problem with this construction: while the amplitude of an individual term connecting sites a distance ℓ apart will still be $\sim D^{-2\ell}$, there are exponentially many such terms so that the total effective amplitude is $\sim 4^\ell D^{-2\ell} \sim \mathcal{O}(1)$. The small parameter in the perturbative construction is lost. Our symbolic calculations do confirm this issue and indeed show that the total effective amplitude is not decaying with the support of the operator in contrast to the non-interacting case. As far as we can tell, this issue is not addressed at all in the proof of MBL by Imbrie [47, 48] which uses the same kind of unitary transformations but seems to be only concerned about resonances. The latter is also a much more severe problem in the interacting case. Even if we assume that the perturbative construction is convergent for carefully chosen disorder configurations without resonances and thermal inclusions due to some miraculous cancellation of contributions stemming from different commutator paths, many-body resonances will destroy the approach when present. A long-range term typically in-

volves operators on all sites between the left most and the right most site. Consequently, the renormalization will involve linear combinations of all the random fields on this cluster and there are exponentially many of such terms. Clearly, the argument for the non-proliferation of resonances made in the non-interacting case is then no longer valid. At the very least, we believe that we have shown that there is no reason to believe that the proof in Refs. [47, 48] is valid. It seems to ignore that, in general, the number of terms connecting distant sites grows exponential with the distance between the sites. No argument is made why the construction remains controlled by a small parameter despite the exponential number of terms and why resonances do not proliferate. Our symbolic calculations for finite chains and finite orders of the transformation suggest that such an argument, in fact, cannot be made and that a perturbative construction of local conserved charges in this way is impossible except for $D = \infty$ where the model is trivially localized.

While we have concentrated here on the Heisenberg chain with quenched disorder, we note that in the attempted proof of MBL by Imbrie [47, 48] the transverse Ising chain with random couplings and fields in considered instead. For the latter model, it has recently been rigorously proven [37] that the norm of a local operator when commuted k -times with the Hamiltonian grows faster than exponential with k and, in fact, asymptotically like the general bound (II.12). Here, we have shown that if a local operator remains quasi-local when commuted with a Hamiltonian then the total norm cannot grow faster than exponential. If we negate this statement, then this means that if the commutator norm of a local operator with a Hamiltonian grows faster than exponential — as in the transverse Ising case — then the commutator is necessarily not a quasi-local operator. It can at best be algebraically localized. I.e., our results come close to proving that the operator growth hypothesis is valid in the strict sense that an almost factorial growth indicates an ergodic systems and that an MBL phase does not exist in the transverse Ising chain. The only assumption we have made is that for the commutator to remain quasi-local, contributions to the connected clusters coming from sites far away from the local operator are exponentially suppressed, see App. A. This seems to be a physical requirement for a localized model. Mathematically it is also hard to see how a local operator can otherwise remain quasi-local. This would then require some miraculous cancellation between different paths which has to happen for *any local operator and most disorder configurations*. For the transverse Ising chain we already know for sure that such destructive interference effects between different paths do not exist because a gauge can be chosen such that all the terms in the commutator are positive [37]. Making these arguments even more rigorous might be the last remaining step in proving that localization is not possible in general in the many-body case.

ACKNOWLEDGMENTS

J.S. acknowledges discussions with D. Sels and M. Kiefer-Emmanouilidis and funding by the NSERC Discovery program and by the DFG via the research unit FOR 2316.

Appendix A: Localized Models

We can strengthen our argument from section II C so that rather than a hard cutoff for contributing connected clusters, we consider contributions from bonds increasingly distant from our original site to decay exponentially. We wish to insert this condition into the counting of connected clusters. To do this, first note that the Stirling number of the second kind can be written as

$$S(k, j) = \sum_{k_0 + \dots + k_{j-1} = k} \frac{1}{j!} \prod_i \frac{1}{a_i!} \binom{k}{k_0, k_1, \dots, k_{j-1}} \quad (\text{A.1})$$

where each k_i is an integer greater than or equal to 1. The term in brackets is the multinomial coefficient which is defined as

$$\binom{k}{k_0, k_1, \dots, k_{j-1}} = \frac{k!}{k_0! k_1! \dots k_{j-1}!}. \quad (\text{A.2})$$

Eq. (A.2) can be interpreted as the number of ways of distributing k objects into j boxes with k_i objects in box i , $0 \leq i \leq j-1$. Unlike the Stirling number of the second kind $S(k, j)$, we are now specifying the number of objects in each of the j boxes, which is why we have the sum in Eq. (A.1). Further, we now account for the order of the boxes; eliminating this constraint leads to the factor of $\frac{1}{j!}$ in Eq. (A.1). Finally, the product of $\frac{1}{a_i!}$ factors corrects for the fact that the multinomial coefficient treats repeated integers in the set $\{k_1, \dots, k_j\}$ as separate cases while $S(k, j)$ does not. To better illustrate this formula, we provide an example of its usage.

Example: Consider $k = 6$, $j = 4$. Then our solutions to $k_1 + \dots + k_j = k$ will involve permutations of $\{k_1, k_2, k_3, k_4\} = \{1, 1, 1, 3\}$ or $\{1, 1, 2, 2\}$. There will be $4! = 24$ terms in the sum for each of these possibilities, but since the multinomial coefficient does not change value when swapping any of the k_i 's, the $\frac{1}{j!}$ factor turns this into a sum of the two multinomial coefficients with $\{k_1, k_2, k_3, k_4\} = \{1, 1, 1, 3\}, \{1, 1, 2, 2\}$. However, we still have the correcting $\frac{1}{a_i!}$ product. There are three repeated integers in the set $\{1, 1, 1, 3\}$ so we take $\prod_i \frac{1}{a_i!} = \frac{1}{3!}$, while there are two sets of two repeated integers in the set $\{1, 1, 2, 2\}$ so we take $\prod_i \frac{1}{a_i!} = \frac{1}{2!2!}$. The r.h.s. of Eq. (A.1) then becomes

$$\frac{1}{3!} \binom{6}{1, 1, 1, 3} + \frac{1}{2!2!} \binom{6}{1, 1, 2, 2} = 65 \quad (\text{A.3})$$

and in fact, $S(6, 4) = 65$.

We now denote by $\tilde{S}(k, j)$ our ‘adjusted’ Stirling number which inserts the requirement that contributions from sites of increasing distance from our initial site are exponentially decaying. Let k_n denote the number of bonds at a distance n from our initial site, where a distance of zero corresponds to a bond involving our initial site. We want exponential decay of the ratio of the contributions from bonds at k_n to bonds at k_0 . To insert this condition, we multiply by a factor of $e^{-nk_n/\xi}$ for each k_n and for any constant $\xi > 0$ which plays the role of a localization length. We note that this is normalized so that at k_0 this factor is 1, meaning the initial site is not reduced. This separate treatment of the k_n ’s, which represent the number of times each bond appears in the connected cluster, is why the form (A.1) of $S(k, j)$ is desirable. Applying the decaying factors, we get

$$\begin{aligned} & \tilde{S}(k, j) \\ &= \sum_{k_0+\dots+k_{j-1}=k} \frac{1}{j!} \prod_i \frac{1}{a_i!} \binom{k}{k_0, \dots, k_{j-1}} \prod_{n=0}^{j-1} e^{-nk_n/\xi} \\ &\leq \sum_{k_0+\dots+k_{j-1}=k} \binom{k}{k_0, \dots, k_{j-1}} \prod_{n=0}^{j-1} \frac{e^{-nk_n/\xi}}{n+1} \\ &= e^{k/\xi} \left(\sum_{n=1}^j \frac{e^{-n/\xi}}{n} \right)^k. \end{aligned} \quad (\text{A.4})$$

We also loosened the condition on the k_i ’s in the second line so that they are now greater than or equal to 0 instead of 1 so that we may apply the multinomial theorem in the third line. Since this may only increase the sum due to allowing more solutions to $k_0 + \dots + k_{j-1} = k$, the upper bound is still valid. For $k \gg j \gg 1$ we can extend the sum up to infinity and obtain

$$\tilde{S}(k, j) \leq \left(-e^{1/\xi} \ln \left(1 - e^{-1/\xi} \right) \right)^k. \quad (\text{A.5})$$

Then the adjusted number of connected clusters, with the inserted requirement of the exponentially decreasing contribution with cluster length, is bounded from above by

$$\begin{aligned} \sum'_{\{I_1, \dots, I_k\}} &= \sum_{j=1}^k 2^j \tilde{S}(k, j) \\ &\leq 2(2^k - 1) \left(-e^{1/\xi} \ln \left(1 - e^{-1/\xi} \right) \right)^k \\ &\approx 2 \left(-2e^{1/\xi} \ln \left(1 - e^{-1/\xi} \right) \right)^k \end{aligned} \quad (\text{A.6})$$

where in the last line we took the large k limit. Defining the constant $\alpha = -2e^{1/\xi} \ln \left(1 - e^{-1/\xi} \right)$, we therefore obtain the bound

$$\| [H, A]^{(k)} \| \leq 2 \| A \| (2\alpha \tilde{J})^k. \quad (\text{A.7})$$

We note that this more careful calculation is qualitatively fully consistent with Eq. (II.21) in the main text where we made the simplifying assumption that clusters longer than the localization length do not contribute at all to the norm. We thus conclude that the norm growth of the commutator in any localized model is at most exponential.

Appendix B: Lieb-Robinson bounds

Another physically relevant property which can be obtained from our results for the k -fold commutator are Lieb-Robinson bounds for the spreading of information in Euclidean time.

1. General bound

We start by summarizing the result for the generic, quantum chaotic case which was first derived in Ref. [30]. We consider the commutator between two local operators a distance ℓ apart

$$\begin{aligned} \| [A_0(\tau), B_\ell(0)] \| &= \| \left[\sum_k [H, A_0]^{(k)} \frac{\tau^k}{k!}, B_\ell \right] \| \quad (\text{B.1}) \\ &\leq 2 \| A \| \| B \| \sum_k \frac{(2CJ\tau)^k}{k!} \sum_{j=\ell}^k 2^j S(k, j) \end{aligned}$$

where we have used the fact that the lattice animal has to consist of at least $j = \ell$ bonds for the commutator to be non-zero. We can now use the representation of the Stirling numbers of the second kind

$$S(k, j) = \sum_{s=1}^j \frac{(-1)^{j-s} s^{k-1}}{(j-s)!(s-1)!} \quad (\text{B.2})$$

to rewrite the bound of the commutator as

$$\begin{aligned} & 2 \| A \| \| B \| \sum_{j=\ell}^{\infty} 2^j \sum_{s=1}^j \frac{(-1)^{j-s}}{s(j-s)!(s-1)!} \underbrace{\sum_{k=1}^{\infty} \frac{(2CJ\tau s)^k}{k!}}_{e^{2CJ\tau s} - 1} \\ &= 2 \| A \| \| B \| \sum_{j=\ell}^{\infty} \frac{(2q)^j}{j!}, \quad q = e^{2CJ\tau} - 1 \quad (\text{B.3}) \\ &= 2 \| A \| \| B \| \frac{e^{2q}}{(l-1)!} \int_0^{2q} x^{\ell-1} e^{-x} dx. \end{aligned}$$

For $\ell \gg q$ we obtain the scaling

$$\begin{aligned} \| [A_0(\tau), B_\ell(0)] \| &\sim 2 \| A \| \| B \| \frac{(2q)^l}{l!} \quad (\text{B.4}) \\ &\sim 2 \| A \| \| B \| (2q)^\ell \left(\frac{e}{\ell} \right)^\ell. \end{aligned}$$

This means that the commutator is $\mathcal{O}(1)$ if $q \sim \ell$ which is equivalent to $\exp(2CJ\tau) \sim \ell$. I.e., in a generic, chaotic

one-dimensional quantum system with short-range interactions, information is spreading exponentially fast in Euclidean time. From the derivation we see that this exponentially fast spreading is directly related to the almost factorial growth of the commutator $[H, A]^{(k)}$.

2. Non-interacting bound

Let us first consider the case without disorder. In this case we have an explicit result for the contribution of lattice animals with j bonds, see Eq. (III.11). Generalizing this to the case of an operator A , we find

$$\begin{aligned} \|[A_0(\tau), B_\ell(0)]\| &\leq 2\|A\|\|B\| \sum_{k=\ell-1}^{\infty} \frac{(4\tau)^k}{k!} \sum_{j=\ell}^{k+1} \binom{k}{\frac{k+1-j}{2}} \\ &= 2\|A\|\|B\| \sum_{k=\ell-1}^{\infty} \frac{(4\tau)^k}{k!} \sum_{j=0}^{(k+\ell)/2} \binom{k}{j} \end{aligned} \quad (\text{B.5})$$

for the case where k is odd, and ℓ is even. This becomes non-zero if $k \gtrsim \ell$ and is of order $\mathcal{O}(1)$ if $\tau \sim \ell$. I.e., for a non-interacting system the spreading is ballistic in Euclidean time. This is directly related to the exponential instead of almost factorial growth of $[H, A]^{(k)}$ which is due to the fact that most lattice animals are zero.

Importantly, this scaling remains intact in the non-interacting disordered case. I.e., the spreading in Euclidean time is still ballistic but the time scale is renormalized. This can be seen by considering

$$\|[A_0(\tau), B_\ell(0)]\| \leq 2\|A\|\|B\| \sum_{k=\ell-1}^{\infty} \frac{(\tau)^k}{k!} \sum_{j=\ell}^{k+1} \underbrace{\|[H, A_0]^{(k)}\|}_{2^{2j-1}\eta^{k-j+1}} \quad (\text{B.6})$$

where we have used that $s_j^{(1)}(k) = \|[H, A_0]_j^{(k)}\| \sim \theta(k - (j-1))2^{2j-1}\eta^{k-j+1}$. I.e., independent of the disorder we always have that $s_j^{(1)}(j-1) = 2^{2j-1}$, see Eq. (III.13). Only the further increase of $s_j^{(1)}(k)$ for $k \geq j-1$ is affected by disorder, $\eta = \eta(D)$. However, this does not affect the scaling when the commutator becomes of order $\mathcal{O}(1)$ which is still given by $\tau \sim \ell$.

3. Many-body localization

In the interacting, disordered case all the paths which exist in the non-disordered case remain present, see Fig. 13. This suggests that information will still spread exponentially fast, $e^\tau \sim \ell$, in Euclidean time albeit with a renormalized time scale. I.e., based on the view of the commutator $[H, A_0]^{(k)}$ as a graph we expect that while the spreading of information does slow down with increasing disorder, this is merely a rescaling of time but the functional form remains unaffected.

The only way how the spreading of information can change qualitatively is if disorder introduces destructive

interferences between different paths in the graph 13. We note again that this is not possible in the transverse Ising model with random fields because the model is stoquastic and all the weights along the edges in the graph can be taken to be positive.

The XXZ chain does not have the stoquastic property so that, in principle, destructive interferences are possible. If we assume this to be the case, then a minimal model is the one discussed in Sec. A where the Stirling numbers of the second kind are replaced by modified Stirling numbers, see Eq. (A.4). I.e., our Lieb-Robinson bound will then be given by Eq. (B.1) with $S(k, j) \rightarrow \tilde{S}(k, j)$. We can then obtain a bound for information spreading by using

$$\tilde{S}(k, j) \leq (-e^{1/\xi} \ln(1 - e^{-1/\xi}))^k \equiv \alpha^k. \quad (\text{B.7})$$

Now the two sums can be performed and we find

$$\begin{aligned} \|[A_0(\tau), B_\ell(0)]\| &\leq \frac{4\|A\|\|B\|}{(\ell-1)!} e^{4CJ\alpha\tau} \\ &\times (\gamma(\ell, 4CJ\alpha\tau) - 2^{\ell-1} e^{-2CJ\alpha\tau} \gamma(\ell, 2CJ\alpha\tau)) \end{aligned} \quad (\text{B.8})$$

where $\gamma(\ell, x)$ is the lower incomplete Gamma function. For large ℓ we can approximate the Gamma function and find

$$\|[A_0(\tau), B_\ell(0)]\| \lesssim \frac{2\|A\|\|B\|}{\ell!} (4CJ\alpha\tau)^\ell \quad (\text{B.9})$$

Using the Stirling approximation this means that the commutator is of order $\mathcal{O}(1)$ if $\tau \sim \ell/(4CJ\alpha\tau)$. This means that the spreading is ballistic and since $\alpha = \alpha(\xi)$ increases with increasing localization length ξ , the velocity decreases with increasing disorder as expected. We stress once more though that we have not found any indications for such destructive interference—which would result in the modified Stirling numbers $\tilde{S}(k, j)$ —to be present in the Heisenberg chain.

To summarize, an almost factorial growth of the commutator $[H, A_0]^{(k)}$, as expected in a generic quantum chaotic system, leads to exponential spreading while an exponential growth leads to ballistic spreading of information in Euclidean time.

Appendix C: Off-diagonal matrix elements

We can also use our bounds on the growth of the commutator $[H, A]^{(k)}$ for a local operator A to derive results for the asymptotic scaling of off-diagonal matrix elements of A in the energy eigenbasis for a finite system.

We have

$$\langle E_i | A(\tau) | E_j \rangle = A_{ij} e^{\omega\tau} \quad (\text{C.1})$$

with $\omega = E_i - E_j$ and $A_{ij} = \langle E_i | A | E_j \rangle$ where $|E_j\rangle$ are energy eigenstates. We note that $|A_{ij}| \leq \sqrt{\text{tr } \mathbb{1}_{M \times M} \|A\|_p} \equiv \|A\|$ where $\|A\|_p$ with $p = 1, 2$ are the norms defined in Eq. (II.4). This implies that

$$|A_{ij}| \leq \|A(\tau)\| e^{-\omega\tau} \quad (C.2)$$

which is valid for any time τ . We can thus minimize the r.h.s. with respect to τ to obtain an optimal bound.

1. General case

The general, quantum chaotic case was already analyzed in Ref. [30]. Here we provide a short summary. From Eq. (B.3) we see that

$$\|A(\tau)\| \leq \|A\| e^{2q}, \quad q = e^{2CJ\tau} - 1. \quad (C.3)$$

Minimizing the function $e^{2q}e^{-\omega\tau}$ w.r.t. τ one finds

$$|A_{ij}| \leq \|A\| \begin{cases} \exp(2\tilde{\omega}(1 - \ln \tilde{\omega}) - 2) & \tilde{\omega} > 1 \\ 1 & \tilde{\omega} \leq 1 \end{cases} \quad (C.4)$$

with $\tilde{\omega} = \omega/(4CJ)$. This means that matrix elements are in general non-zero even for extensive energy differences ω . Asymptotically, these matrix elements decay faster than exponential.

2. Non-interacting case

In the non-interacting case, energy differences ω cannot be extensive. A more precise bound can be obtained by using again Eq. (C.2) together with the bound

$$\|A(\tau)\| \leq \sum_k \frac{\tau^k}{k!} \underbrace{\|[H, A]^{(k)}\|}_{\leq \|A\|(8CJ)^k} \quad (C.5)$$

where we have used Eq. (II.17). This leads to the upper bound

$$|A_{ij}| \leq \|A\| \exp[(8cJ - \omega)\tau]. \quad (C.6)$$

Minimizing the r.h.s. we thus find $|A_{ij}| = 0$ if $\omega > 8cJ$ and the generic bound $|A_{ij}| \leq \|A\|$ if $\omega \leq 8cJ$.

In the disordered, non-interacting case a sharp cut-off will remain. To be concrete, we can for example consider the σ^z operator in the Anderson case. Using Eq. (C.5) together with the bound (III.15) we find

$$\begin{aligned} |\sigma_{ij}^z| &= 0, & \omega &> 8(D+1) \\ |\sigma_{ij}^z| &\leq \frac{1}{D+1}, & \omega &\leq 8(D+1) \end{aligned} \quad (C.7)$$

In addition to the sharp cut-off in energy, we also find a non-trivial bound for the magnitude of the matrix elements below that cutoff in this case which is consistent with the fact that the eigenstates of the Anderson model are eigenstates of σ^z for $D \rightarrow \infty$. Off-diagonal matrix elements therefore vanish entirely in this limit.

3. Many-body localization

As for the Lieb-Robinson bounds, the general result (C.4) will still apply qualitatively as long as $[H, A]^{(k)}$ does grow almost factorially. We know this to be the case for the transverse Ising model with random fields and found strong evidence that this is also true in the disordered Heisenberg model.

We can, however, check again what would happen if there are destructive interferences between different paths in the commutator graph, leading to our model with the modified Stirling numbers $\tilde{S}(k, j)$, see Eq. (A.6). Using the bound (C.5) with $\|[H, A]^{(k)}\| \leq (2CJ)^k \|A\| \sum'_{I_1, \dots, I_k} \leq 2(4CJ\alpha)^k \|A\|$ with $\alpha = -e^{1/\xi} \ln(1 - e^{-1/\xi})$ we find

$$\|A(\tau)\| \leq 2\|A\| \exp(4CJ\alpha\tau) \quad (C.8)$$

This then implies

$$\begin{aligned} |A_{ij}| &= 0, & \omega &> 4CJ\alpha \\ |A_{ij}| &\leq \|A\|, & \omega &\leq 4CJ\alpha. \end{aligned} \quad (C.9)$$

It is instructive to consider the limits of weak and strong disorder. For weak disorder, the norm of the local Hamiltonian scales as $\|h\| \sim CJ \sim 1$ if we set the exchange couplings to be of order $\mathcal{O}(1)$. For the parameter α we find that $\alpha \sim \ln \xi$ for $\xi \gg 1$. This means that there is no cut-off for $\xi \rightarrow \infty$; extensive energy differences are allowed, qualitatively consistent with the general bound (C.4). For very strong disorder, on the other hand, $\|h\| \sim CJ \sim D$ where D is the disorder strength. The parameter α for $\xi \ll 1$ becomes $\alpha \sim 1$. For very strong disorder in a finite system the prediction of this model is therefore that a sharp cut-off of order $4D$ exists. This is consistent with the infinite disorder limit where the eigenstates are Ising states and local operators can at most couple states which differ by a local spin flip.

To summarize, an almost factorial growth of the commutator $[H, A]^{(k)}$ implies that matrix elements are non-zero even for extensive energy differences but that they decay faster than exponential with the magnitude of the energy difference. For an exponential growth, on the other hand, there is a sharp cut-off and matrix elements for states with an energy difference larger than this cut-off are zero.

Appendix D: Graphs

The growth of the 1-norm of the commutator $[H, \sigma_0^z]^{(k)}$ can also be understood using graphs both without and with disorder. Here we provide some more details how such graphs can be constructed and how they have to be read.

1. No disorder

We use a rooted, directed, weighted, infinite graph to model the commutator growth. In the graph, each node represents classes of terms formed by the commutator and each directed edge represents connections between classes of terms formed via commutation with the Hamiltonian. For example, if commuting a term of class A with H produces a term of class B then an arrow is drawn on the graph from A to B . Further, the 1-norm of terms of class B in that commutation is assigned to the weight of that edge. The classes are organized such that each term of that class produces the same result when commuting with H .

In the non-interacting, non-disordered case, whose exact commutator structure is given by Eq. (III.4) and Eq. (III.5), we find that the growth is modelled by the left column of the graph of Fig. 4. By convention, we label the classes by the string of Pauli operators beginning with σ^x , and we omit index labels with the understanding that a string of operators acts on consecutive sites. Note that terms are invariant with respect to commutation with H under the transformation $\sigma^x \leftrightarrow \sigma^y$, so we group terms of the form $\sigma^x \cdots \sigma^y$ and $\sigma^y \cdots \sigma^x$ into the same class, and $\sigma^x \cdots \sigma^x$ and $\sigma^y \cdots \sigma^y$, but not $\sigma^x \cdots \sigma^y$ and $\sigma^x \cdots \sigma^x$.

Enumerative calculations on the graph Fig. 4 now allow us to calculate the 1-norm growth and spatial structure of the commutator $[H, \sigma_0^z]^{(k)}$. We always begin with a single σ^z operator which we label node 1. We then commute with the Hamiltonian k times which corresponds to a walk of length k on the graph starting at node 1. To get the total 1-norm, we must sum over all weighted walks of length k which begin at node 1 with no restrictions on the end node. By a weighted walk we mean a walk through the edges of the graph in which the running count is multiplied by the weight of the traversed edge.

It is simple to count the total number of weighted walks on the graph Fig. 4 for $D = 0$ (left column) if we make the following observation. If on the i -th step we are at node 1, then we have a single option for the next node, and this traversal has weight 8. Thus, the weighted number of options is $8 \cdot 1 = 8$. If we are at any other node, there are two options for the next node, and each traversal has weight 4, so the weighted number of options is $4 \cdot 2 = 8$. Since the number of weighted options is thus equal at each step and there are k total steps, the 1-norm must be equal to 8^k , reproducing our result of Eq. (III.8).

We label node l to be the node corresponding to the class of terms which are a string of l Pauli matrices. The support on l sites then corresponds to the weighted number of walks which begin at node 1 and end at node l . We first consider the support on one site. We note that any walk that begins and ends at node 1 on the graph Fig. 4 must have even k and traces out a Dyck path. Thus, the total unweighted number of walks is equal to $C\left(\frac{k}{2}\right)$, where $C(n)$ in this case is the Catalan number. However, due to the edge leaving the first node having a different

weight, to find the total weighted number of Dyck paths one must use the following formula

$$s_1^{(1)}(k) = \sum_m w(m, k) p(m, k) \quad (\text{D.1})$$

where $s_1^{(1)}(k)$ means the 1-norm of terms with support on one site as a function of k , $w(m, k)$ is the weight of a path as a function of m and k where m is the number of traversals of the single edge of weight 8, and $p(m, k)$ is the number of paths as a function of m and k . Note that we use the term paths instead of walks here to refer to the fact that these are Dyck paths. It is clear that the bounds on m are $1 \leq m \leq \frac{k}{2}$ and that $w(m, k) = 4^{k-m} 8^m = 4^k 2^m$. We calculate $p(m, k)$ by partitioning the Dyck path into m parts according to intersections with the x -axis. We then have

$$\begin{aligned} p(m, k) &= \sum_{i_1+...+i_m=\frac{k}{2}} \prod_{j=1}^m C(i_j - 1) \\ &= \frac{m}{k-m} \binom{k-m}{\frac{k}{2}} \end{aligned} \quad (\text{D.2})$$

where we used Catalan's k -fold convolution formula. This leads to

$$s_1^{(1)}(k) = 4^k \sum_{m=1}^{\frac{k}{2}} 2^m \frac{m}{k-m} \binom{k-m}{\frac{k}{2}} = 4^k \binom{k}{\frac{k}{2}}. \quad (\text{D.3})$$

The support on 2 sites is then easily found using a recursive strategy as

$$s_2^{(1)}(k) = \frac{1}{4} s_1(k+1) = 2^{2k+1} \binom{k}{\frac{k-1}{2}}. \quad (\text{D.4})$$

We see that this reproduces our previous result Eq. (III.11) with $l = 2$. Another recursive equation gives the support on 3 sites

$$\begin{aligned} s_3^{(1)}(k) &= \frac{1}{4} s_2(k+1) - 2s_1(k) \\ &= 2^{2k+1} \left[\binom{k+1}{\frac{k}{2}} - \binom{k}{\frac{k}{2}} \right] = 2^{2k+1} \binom{k}{\frac{k-2}{2}}. \end{aligned} \quad (\text{D.5})$$

We see that this also agrees with our previous result Eq. (III.11) for $l = 3$. Finally, we get the following recursive equation for $l \geq 4$:

$$s_l^{(1)}(k) = \frac{1}{4} s_{l-1}(k+1) - s_{l-2}(k). \quad (\text{D.6})$$

Simple inductive arguments show that the solution to Eq. (D.6) with base cases (D.4) and (D.5) is indeed our previous result (III.11).

2. Disordered case

In the disordered case, we find that we have new classes of terms in the commutator with edges given by the magnetic field values h_j . For the Anderson case, we know that

$h_j \in [-D, D]$, so the maximum absolute value of the disorder at each site is D . For the Aubry-André model, the same additional terms in the commutator appear but in this case the maximum value is $\lambda/2$. This allows us to create a modified graph which contains an additional column of terms, see Fig. 4, and which allows us to derive again an upper bound of the 1-norm. We discuss the Anderson case here and note that the Aubry-André case follows immediately with the replacement $D \rightarrow \lambda/2$.

Since D is an upper bound on the disorder at each site, we can only compute an upper bound on the 1-norm growth of the commutator. Following the same strategy as for the non-disordered case, we see that at a given step, if we are at node 1, then we have a weighted number of options of 8. If we are at the $\sigma^x \sigma^x$ node, we have a weighted number of options of $4 + 8D$. If we are at any other node, we have a weighted number of options of $8 + 8D$. The maximum of these is $8 + 8D$, so we get the following upper bound on the 1-norm growth of the commutator, keeping in mind that the first step must have a contribution of 8:

$$\| [H, \sigma_0^z] \|_1 \leq 8^k (D + 1)^{k-1}. \quad (\text{D.7})$$

This is the result Eq. (III.15). The bound is exponential as expected, with an increasing disorder strength corresponding to an increased growth rate. We also see that setting $D = 0$ gives us 8^k , the exact result in the case without disorder.

Now we consider the spatial structure of the commutator. We can get a qualitative sense of why localization occurs in this case. Recall that the support on l sites in the graphical language is the weighted number of walks of length k that start at node 1 and ends at node l . First note that in this case there are two nodes for each l . Additionally, with the new terms due to disorder, there will be more possible walks of length k as one may also traverse the edges with weight $8D$. However, traversing these edges does not result in a node with an increased l . Therefore, in contrast to the non-disordered case, there will be a greater number of walks that end at nodes with smaller l , and the relative number of walks should decrease as l increases. Furthermore, for $D \gg 1$ traversing the edges with weight $8D$, which does not increase l , leads to a much larger contribution to the norm than traversing those edges which connect nodes with different l 's. This means that the 1-norm of term with support on l sites decays with l , indicating localization.

For a more quantitative analysis, let us consider the upper bound on the support at l sites $s_l^{(1)}(k)$. Numerical calculations using weighted adjacency matrices led to the following result for the support on one site

$$\begin{aligned} s_1^{(1)}(k) &\leq 2^{3k-1} D^{k-2} \sum_{i=0}^{\frac{k-2}{2}} C(i) \binom{k-1}{2i} (2D)^{-2i} \quad (\text{D.8}) \\ &= 2^{3k-1} D^{k-2} {}_2F_1 \left(\frac{1-k}{2}, \frac{2-k}{2}; 2; \frac{1}{D^2} \right) \end{aligned}$$

where ${}_2F_1$ is the hypergeometric function. Note that this result is derived for even k . For k odd the support will be zero; one can infer this from Fig. 4 since there is no possible walk on the graph beginning and ending at the top node with an odd number of steps. The upper bound in Eq. (D.8) only arises from the fact that D is an upper bound on the local magnetic fields; the enumerative calculations are exact. Similar numerical calculations show that the support on $l > 1$ sites is bounded from above by a hypergeometric function as well but with a different leading term

$$\begin{aligned} s_l^{(1)}(k) &\leq 2^{3k+2-l} \binom{k-1}{l-2} D^{k-l+1} \quad (\text{D.9}) \\ &\times {}_2F_1 \left(\frac{1-k}{2}, \frac{2-k}{2}; 2; \frac{1}{D^2} \right). \end{aligned}$$

The upper bound is looser in this case because the enumerative calculations are no longer exact. We are then interested in the ratio $s_l^{(1)}(k)/s_1^{(1)}(k)$ in the limit $k \gg l \gg 1$. Since the upper bound given for $s_l^{(1)}(k)$ is in fact looser than that given for $s_1^{(1)}(k)$, we may bound the ratio by the ratio of the two given upper bounds, leading to the result

$$\begin{aligned} \frac{s_l^{(1)}(k)}{s_1^{(1)}(k)} &\leq \binom{k-1}{l-2} (2D)^{3-l} \\ &\approx \frac{1}{\sqrt{2\pi l}} \left(\frac{ke}{l} \right)^l e^{-\frac{l^2}{2k}} (2D)^{3-l} \quad (\text{D.10}) \end{aligned}$$

This coincides with Eq. (III.18). As mentioned in the main text, there is a maximum in this ratio which shifts to larger l with increasing k , which is not expected for a localized model. This is likely explained by the looseness of the bound Eq. (D.9); while it is correct for the leading term in D , the actual prefactors for terms of decreasing order in D become increasingly smaller than those in the given bound. We expect that a formula replacing Eq. (D.9) in which the enumerative calculations are exact and the upper bound only comes from D would not possess this unexpected behaviour, although we have been unable to derive such a formula. We nevertheless see the expected result that with k held constant we have an exponential decay of the ratio of support for increasing l , and that increasing D corresponds to an increasing rate of decay.

[1] P. W. Anderson, Absence of diffusion in certain random lattices, Phys. Rev. **109**, 1492 (1958).

[2] J. T. Edwards and D. J. Thouless, Numerical studies of localization in disordered systems, J. Phys. C **5**, 807

(1972).

[3] E. Abrahams, P. W. Anderson, D. C. Licciardello, and T. V. Ramakrishnan, Scaling theory of localization: Absence of quantum diffusion in two dimensions, *Phys. Rev. Lett.* **42**, 673 (1979).

[4] E. Abrahams, ed., *50 Years of Anderson Localization* (World Scientific, Singapore, 2010).

[5] D. M. Basko, I. L. Aleiner, and B. L. Altshuler, Metal-insulator transition in a weakly interacting many-electron system with localized single-particle states, *Ann. Phys.* **321**, 1126 (2006).

[6] M. Žnidarič, T. Prosen, and P. Prelovšek, Many-body localization in the heisenberg xxz magnet in a random field, *Phys. Rev. B* **77**, 064426 (2008).

[7] V. Oganesyan and D. A. Huse, Localization of interacting fermions at high temperature, *Phys. Rev. B* **75**, 155111 (2007).

[8] A. Pal and D. A. Huse, Many-body localization phase transition, *Phys. Rev. B* **82**, 174411 (2010).

[9] J. H. Bardarson, F. Pollmann, and J. E. Moore, Unbounded growth of entanglement in models of many-body localization, *Phys. Rev. Lett.* **109**, 017202 (2012).

[10] D. J. Luitz, N. Laflorencie, and F. Alet, Many-body localization edge in the random-field heisenberg chain, *Phys. Rev. B* **91**, 081103 (2015).

[11] D. J. Luitz, N. Laflorencie, and F. Alet, Extended slow dynamical regime close to the many-body localization transition, *Phys. Rev. B* **93**, 060201 (2016).

[12] M. Serbyn, Z. Papić, and D. A. Abanin, Local conservation laws and the structure of the many-body localized states, *Phys. Rev. Lett.* **111**, 127201 (2013).

[13] R. Vosk, D. A. Huse, and E. Altman, Theory of the many-body localization transition in one-dimensional systems, *Phys. Rev. X* **5**, 031032 (2015).

[14] E. Altman and R. Vosk, Universal dynamics and renormalization in many-body-localized systems, *Annual Review of Condensed Matter Physics* **6**, 383 (2015).

[15] E. V. H. Doggen, F. Schindler, K. S. Tikhonov, A. D. Mirlin, T. Neupert, D. G. Polyakov, and I. V. Gornyi, Many-body localization and delocalization in large quantum chains, *Phys. Rev. B* **98**, 174202 (2018).

[16] P. Sierant, D. Delande, and J. Zakrzewski, Thouless time analysis of anderson and many-body localization transitions, *Phys. Rev. Lett.* **124**, 186601 (2020).

[17] R. Nandkishore and D. A. Huse, Many-body localization and thermalization in quantum statistical mechanics, *Annual Review of Condensed Matter Physics* **6**, 15 (2015).

[18] A. C. Potter, R. Vasseur, and S. A. Parameswaran, Universal properties of many-body delocalization transitions, *Phys. Rev. X* **5**, 031033 (2015).

[19] D. A. Huse, R. Nandkishore, and V. Oganesyan, Phenomenology of fully many-body-localized systems, *Phys. Rev. B* **90**, 174202 (2014).

[20] J. Suntajs, J. Bonca, T. Prosen, and L. Vidmar, Quantum chaos challenges many-body localization, *Phys. Rev. E* **102**, 062144 (2020).

[21] J. Suntajs, J. Bonca, T. Prosen, and L. Vidmar, Ergodicity breaking transition in finite disordered spin chains, *Phys. Rev. B* **102**, 064207 (2020).

[22] M. Kiefer-Emmanouilidis, R. Unanyan, J. Sirker, and M. Fleischhauer, Bounds on the entanglement entropy by the number entropy in non-interacting fermionic systems, *SciPost Phys.* **8**, 083 (2020).

[23] M. Kiefer-Emmanouilidis, R. Unanyan, M. Fleischhauer, and J. Sirker, Evidence for unbounded growth of the number entropy in many-body localized phases, *Phys. Rev. Lett.* **124**, 243601 (2020).

[24] M. Kiefer-Emmanouilidis, R. Unanyan, M. Fleischhauer, and J. Sirker, Slow delocalization of particles in many-body localized phases, *Phys. Rev. B* **103**, 024203 (2021).

[25] M. Kiefer-Emmanouilidis, R. Unanyan, M. Fleischhauer, and J. Sirker, Unlimited growth of particle fluctuations in many-body localized phases, *Annals of Physics* **168481** (2021).

[26] M. Kiefer-Emmanouilidis, R. Unanyan, M. Fleischhauer, and J. Sirker, Particle fluctuations and the failure of simple effective models for many-body localized phases, *SciPost Phys.* **12**, 034 (2022).

[27] M. Kiefer-Emmanouilidis, R. Unanyan, M. Fleischhauer, and J. Sirker, Comment on "Resonance-induced growth of number entropy in strongly disordered systems", arXiv: 2203.06689 (2022).

[28] D. Sels and A. Polkovnikov, Dynamical obstruction to localization in a disordered spin chain, *Phys. Rev. E* **104**, 054105 (2021).

[29] T. LeBlond, D. Sels, A. Polkovnikov, and M. Rigol, Universality in the onset of quantum chaos in many-body systems, *Phys. Rev. B* **104**, L201117 (2021).

[30] A. Avdoshkin and A. Dymarsky, Euclidean operator growth and quantum chaos, *Phys. Rev. Res.* **2**, 043234 (2020).

[31] D. E. Parker, X. Cao, A. Avdoshkin, T. Scaffidi, and E. Altman, A universal operator growth hypothesis, *Phys. Rev. X* **9**, 041017 (2019).

[32] R. Heveling, J. Wang, and J. Gemmer, Numerically probing the universal operator growth hypothesis, *Phys. Rev. E* **106**, 014152 (2022).

[33] L. D'Alessio, Y. Kafri, A. Polkovnikov, and M. Rigol, From quantum chaos and eigenstate thermalization to statistical mechanics and thermodynamics, *Adv. Phys.* **65**, 239 (2016).

[34] T. LeBlond, K. Malayya, L. Vidmar, and M. Rigol, Entanglement and matrix elements of observables in interacting integrable systems, *Phys. Rev. E* **100**, 062134 (2019).

[35] E. Lieb, and D.W. Robinson, The finite group velocity of quantum spin systems, *Commun. Math. Phys.* **28**, 251 (1972).

[36] S. Bravyi, M.B. Hastings, and F. Verstraete, Lieb-Robinson Bounds and the Generation of Correlations and Topological Quantum Order, *Phys. Rev. Lett* **97**, 050401 (2006).

[37] X. Cao, A statistical mechanism for operator growth, *Journal of Physics A: Mathematical and Theoretical* **54**, 144001 (2021).

[38] C. Fieker, W. Hart, T. Hofmann, and F. Johansson, Nemo/Hecke: Computer algebra and number theory packages for the Julia programming language, in *Proceedings of the 2017 ACM on International Symposium on Symbolic and Algebraic Computation*, ISSAC '17 (Association for Computing Machinery, New York, NY, USA, 2017) p. 157-164.

[39] D. Dominici, Asymptotic analysis of the bell polynomials by the ray method, *Journal of Computational and Applied Mathematics* **233**, 708 (2009), 9th OPSFA Conference.

[40] V.E. Kravtsov, I.M. Khaymovich, E. Cuevas, and M. Amini, A random matrix model with localization and

ergodic transitions, *New J. Phys.* **17**, 122002 (2015).

[41] V.E. Kravtsov, B.L. Altshuler, and L.B. Ioffe, Non-ergodic delocalized phase in Anderson model on Bethe lattice and regular graph, *Ann. Phys.* **389**, 148 (2018).

[42] D. Sels, Bath-induced delocalization in interacting disordered spin chains, *Physical Review B* **106**, L020202 (2022).

[43] S. Aubry and G. André, Analyticity breaking and anderson localization in incommensurate lattices, *Ann. Israel Phys. Soc.* **3**, 18 (1980).

[44] S. Y. Jitomirskaya, Metal-insulator transition for the almost mathieu operator, *Annals of Mathematics* **150**, 1159 (1999).

[45] H. Bethe, *Z. Phys.* **71**, 205 (1931).

[46] F. H. L. Essler, H. Frahm, F. Göhmann, A. Klümper, and V. E. Korepin, *The One-Dimensional Hubbard model* (Cambridge University Press, Cambridge, 2005).

[47] J. Z. Imbrie, Diagonalization and many-body localization for a disordered quantum spin chain, *Phys. Rev. Lett.* **117**, 027201 (2016).

[48] J. Imbrie, On Many-Body Localization for Quantum Spin Chains, *Jour. Stat. Phys.* **163**, 998 (2016).

[49] A. Morningstar, D. A. Huse, and J. Z. Imbrie, Many-body localization near the critical point, *Phys. Rev. B* **102**, 125134 (2020).

[50] J. Z. Imbrie, V. Ros, and A. Scardicchio, Local integrals of motion in many-body localized systems, *Annalen der Physik* **529**, 1600278 (2017).

[51] B. Lu, C. Bertoni, S. J. Thomson, and J. Eisert, Measuring out quasi-local integrals of motion from entanglement (2023), arXiv:2301.01787 [cond-mat.dis-nn].

[52] S. J. Thomson and M. Schirò, Local integrals of motion in quasiperiodic many-body localized systems, *SciPost Phys.* **14**, 125 (2023).

[53] J. R. Schrieffer and P. A. Wolff, Relation between the anderson and kondo hamiltonians, *Phys. Rev.* **149**, 491 (1966).

[54] S. Bravyi, D. P. DiVincenzo, and D. Loss, Schrieffer-wolff transformation for quantum many-body systems, *Annals of Physics* **326**, 2793 (2011).

[55] J. Sirker, Transport in one-dimensional integrable quantum systems, *SciPost Phys. Lect. Notes* , 17 (2020).

[56] A. Morningstar, L. Colmenarez, V. Khemani, D. J. Luitz, and D. A. Huse, Avalanches and many-body resonances in many-body localized systems, *Phys. Rev. B* **105**, 174205 (2022).

[57] H. Ha, A. Morningstar, and D. A. Huse, Many-body resonances in the avalanche instability of many-body localization, *Phys. Rev. Lett.* **130**, 250405 (2023).

[58] D. Sels and A. Polkovnikov, Thermalization of dilute impurities in one-dimensional spin chains, *Phys. Rev. X* **13**, 011041 (2023).

[59] J. C. Peacock and D. Sels, Many-body delocalization from embedded thermal inclusion, *Physical Review B* **108**, 1020201 (2023).